Synthesis, Characterization, Isomerization, and Reactivity of Dimeric Cyclopentadienylnickel Amido Complexes

Patrick L. Holland, Richard A. Andersen,* and Robert G. Bergman*

Contribution from the Department of Chemistry, University of California, Berkeley, California 94720

Received August 21, 1995[⊗]

Abstract: The first cyclopentadienylnickel amido complexes have been isolated and characterized as $[(\eta\text{-}C_5Me_4R')Ni(\mu\text{-}NHR)]_2$ (R = Ph, *p*-tol, 2,6-xyl, ^{t}Bu; R′ = Me, Et). These complexes are dimers in solution and in the solid state, as shown by the synthesis of mixed amido complexes, by NMR spectroscopy, and by crystallographic studies on *cis*-$[Cp^{Et}Ni(\mu\text{-}NH(p\text{-tol}))]_2$ (*cis*-**1′**), *trans*-$[Cp^{Et}Ni(\mu\text{-}NH(2,6\text{-xylyl}))]_2$ (*trans*-**3′**), and *cis*-$[Cp^{Et}Ni(\mu\text{-}NH^tBu)]_2$ (**4′**) ($Cp^{Et} = \eta\text{-}C_5Me_4Et$). Resonances in the ^{1}H NMR spectra of these diamagnetic dimers display unusual chemical shifts that are explained on the basis of ring-current anisotropy and inductive effects. The dimers undergo reversible cis/trans isomerization at elevated temperatures; mechanistic studies indicate that this process proceeds through cleavage of one dative nitrogen−nickel bond, rate-limiting rotation of the amido group, and recoordination to regenerate the bridge. Dimethylzirconocene was essential as a scavenger for trace water in these studies. The dimer $[Cp^*Ni(\mu\text{-}NH(p\text{-tol}))]_2$ (**1**) reacts with CO and with ^{t}BuNC to give the insertion products $Cp^*Ni(CO)(C(O)NH(p\text{-tol}))$ (**6**) and $Cp^*Ni(CN^tBu)(C(N^tBu)NH(p\text{-tol}))$ (**7**), respectively, and with PMe_3 to give the unstable monomeric amido complex $Cp^*Ni(PMe_3)(NH(p\text{-tol}))$ (**5**).

Introduction

There is ample reason to believe that amido, imido, alkoxo, hydroxo, and oxo complexes of the "late" (groups 8−10) transition metals will be reactive.[1] On the basis of HSAB (hard−soft acid−base theory) arguments, a mismatch exists between the "hard" anionic base and the "soft" low-valent late-transition-metal center, resulting in a relatively weak M−N bond. Alternatively, using orbital arguments, nonbonding interactions between filled orbitals on the metal and on the ligand lead to destabilization.[2] The weakness predicted for this bond is expected to lead to high reactivity in both stoichiometric and catalytic reactions.

For this reason, our groups have synthesized amido and imido complexes of the d^6 metals Ru(II),[3] Os(II),[4] and Ir(III)[5] and probed their exchange, elimination, and insertion reactions. In this contribution, these metal−amido studies are extended to a d^8 metal center. Simple amido complexes of Ni(II), Pd(II), and Pt(II) have usually been synthesized by metathesis of a platinum−metal halide or pseudo-halide with an alkali metal amide[6] or by deprotonation of coordinated amines,[7] although imide insertion,[8] β-attack on coordinated imines,[9] and fragmentation of a tetrazenide[10] have also been used. While these syntheses provide many examples of palladium and platinum amides, nickel amides are much less common. At the start of this work, no cyclopentadienylnickel amides were known. We believed, however, that the pentamethylcyclopentadienyl ligand (Cp*) would provide a stabilizing steric influence to allow the isolation of stable amidonickel(II) complexes. This expectation has now been realized: this paper describes nickel amides of the type $[Cp^*Ni(\mu\text{-}NHR)]_2$ along with their solid state stuctures, solution properties, and reactivity.

Results and Discussion

Synthesis of Amido Complexes. A synthetic precursor to Cp* complexes of nickel, Cp*Ni(acac) (acac = *O*,*O*-η^2-acetylacetonate) has been described by Manriquez, but has found surprisingly little use as a route to Cp*Ni(L)(X) complexes (L = neutral ligand, X = anionic ligand).[11,12] The red Cp*Ni(acac) can be synthesized easily in one step from $MgCp^*_2$ and commercially available $[Ni(acac)_2]_n$, using a modified preparation.[12]

Addition of THF to a mixture of Cp*Ni(acac) and the appropriate lithium amide at −40 or −78 °C gave dimeric amido

[⊗] Abstract published in *Advance ACS Abstracts,* January 1, 1996.

(1) For reviews on the subject, see: (a) Bryndza, H. E.; Tam, W. *Chem. Rev.* **1988**, *88*, 1163. (b) Fryzuk, M. D.; Montgomery, C. D. *Coord. Chem. Rev.* **1989**, *95*, 1.

(2) Mayer, J. M. *Comments Inorg. Chem.* **1988**, *8*, 125.

(3) (a) Hartwig, J. F.; Andersen, R. A.; Bergman, R. G. *Organometallics* **1991**, *10*, 1875. (b) Michelman, R. I. Ph.D. Thesis, University of California, Berkeley, 1993.

(4) (a) Michelman, R. I.; Andersen, R. A.; Bergman, R. G. *Organometallics* **1993**, *12*, 2741. (b) Michelman, R. I.; Ball, G. E.; Bergman, R. G.; Andersen, R. A. *Organometallics* **1994**, *13*, 869.

(5) (a) Glueck, D. S.; Bergman, R. G. *Organometallics* **1991**, *10*, 1479. (b) Glueck, D. S.; Winslow, L. J. N.; Bergman, R. G. *Organometallics* **1991**, *10*, 1462. (c) Glueck, D. S.; Wu, J.; Hollander, F. W.; Bergman, R. G. *J. Am. Chem. Soc.* **1991**, *113*, 2041. (d) Dobbs, D. A.; Bergman, R. G. *J. Am. Chem. Soc.* **1993**, *115*, 3836.

(6) (a) Fryzuk, M. D.; MacNeil, P. A.; Rettig, S. J.; Secco, A. S.; Trotter, J. *Organometallics* **1982**, *1*, 918. (b) Bartlett, R. A.; Chen, H.; Power, P. P. *Angew. Chem. Int. Ed. Engl.* **1989**, *28*, 316. (c) Bradley, D. C.; Hursthouse, M. B.; Smallwood, R. J.; Welch, A. J. *Chem. Commun.* **1972**, 872. (d) Power, P. P. *Comments Inorg. Chem.* **1989**, *8*, 177 and references therein. (e) Okeya, S.; Yoshimatsu, H.; Nakamura, Y.; Kawaguchi, S. *Bull. Chem. Soc. Jpn.* **1982**, *55*, 483. (f) Tenten, A.; Jacobs, H. *Z. Anorg. Allg. Chem.* **1991**, *604*, 113. (g) Villanueva, L. A.; Abboud, K. A.; Boncella, J. M. *Organometallics* **1994**, *13*, 3921. (h) Cowan, R. L.; Trogler, W. C. *J. Am. Chem. Soc.* **1989**, *111*, 4750. (i) Seligson, A. L.; Cowan, R. L.; Trogler, W. C. *Inorg. Chem.* **1991**, *30*, 3371. (j) Driver, M. S.; Hartwig, J. F. *J. Am. Chem. Soc.* **1995**, *117*, 4708. (k) Hope, H.; Olmstead, M. M.; Murray, B. D.; Power, P. P. *J. Am. Chem. Soc.* **1985**, *107*, 712. (l) Cetinkaya, B.; Hitchcock, P. B.; Lappert, M. F.; Misra, M. C.; Thorne, A. J. *J. Chem. Soc., Chem. Commun.* **1984**, 148. (m) Rahim, M.; Bushweller, C. H.; Ahmed, K. J. *Organometallics* **1994**, *13*, 4952.

(7) See ref 1b and: (a) Kita, M.; Nonoyama, M. *Polyhedron* **1993**, *12*, 1027. (b) Alcock, N. W.; Bergamini, P.; Kemp, T. J.; Pringle, P. G. *J. Chem. Soc., Chem. Commun.* **1987**, 235. (c) Park, S.; Rheingold, A. L.; Roundhill, D. M. *Organometallics* **1991**, *10*, 615.

(8) (a) Matsunaga, P. T.; Hess, C. R.; Hillhouse, G. L. *J. Am. Chem. Soc.* **1994**, *116*, 3665. (b) Pizzotti, M.; Cenini, S.; Porta, F.; Beck, W.; Erbe, J. *J. Chem. Soc., Dalton Trans.* **1978**, 1155. (c) Beck, W.; Bauder, M. *Chem. Ber.* **1970**, *103*, 583.

(9) Villanueva, L. A.; Abboud, K.; Boncella, J. M. *Organometallics* **1991**, *10*, 2969.

(10) Lee, S. W.; Trogler, W. C. *Inorg. Chem.* **1990**, *29*, 1099.

(11) Bunel, E. E.; Valle, L.; Manriquez, J. M. *Organometallics* **1985**, *4*, 1680.

(12) Smith, M. E.; Andersen, R. A. Submitted for publication.

0002-7863/96/1518-1092$12.00/0

Scheme 1

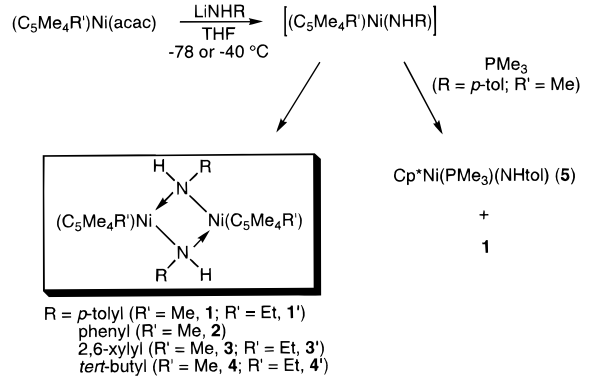

complexes $[Cp^*Ni(\mu\text{-}NHR)]_2$ (R = *p*-tolyl (**1**), phenyl (**2**), 2,6-xylyl (**3**), *tert*-butyl (**4**)) (Scheme 1). In the cases of **1** and **2**, the initial green-blue solution observed at low temperature turned brown as the mixture was warmed or the solvent was removed; workup gave **1** or **2** as purple solids in 60−70% yield. When synthesizing **3** or **4**, allowing the reaction mixtures to warm to room temperature resulted in extensive decomposition. However, removal of solvent at low temperature gave residues from which purple (**3**) or black (**4**) crystals could be obtained in reasonable yields. Dimer **3** was less soluble than **1** or **2**, and could be crystallized from a mixture of toluene and pentane. Compound **4**, on the other hand, was extremely soluble in nonpolar solvents. Crystallization from acetonitrile (in which the crude product is poorly soluble) proved to be a high-yield purification technique for **4**. Each of these nickel amides was highly air and water sensitive in the solid state or in solution.

Since alkylamides of group 10 metals are not very stable,[1,6g,13] it is notable that **4** was isolable. However, the lower stability of alkylamides relative to arylamides was reflected in the thermal stabilities of **1**-**4** in solution: the arylamides **1**-**3** were stable in solution to 80−90 °C (with rigorous exclusion of water and air, as demonstrated below), while **4** decomposed within hours in solution at 45 °C or within 1 day at room temperature.

Analogous procedures led to representative ethyltetramethylcyclopentadienyl (Cp^{Et}) analogues of **1**−**4**. The products **1′**, **3′**, and **4′** (as well as the precursors $MgCp^{Et}_2$ and $Cp^{Et}Ni(acac)$) were more soluble than their Cp* analogues in hydrocarbon solvents, and invariably gave higher-quality crystals. The isolated yields of **1′**, **3′**, and **4′** were generally lower than for the Cp* analogues, due to their high solubilities in common solvents. Spectroscopically, however, they behaved very similarly to **1**, **3**, and **4**, and we shall assume that our crystallographic and spectroscopic findings on the Cp^{Et} compounds are also applicable to their Cp* analogues.[14]

The following three sections of this paper will be devoted to showing that complexes **1**−**4** and **1′**−**4′** are dimers, based on evidence from NMR spectroscopy, variable-temperature phenomena, and X-ray crystallography. It is reasonable to believe that the formation of these dimers proceeds through initial formation of an unsaturated monomeric amido complex Cp*NiNHR; this is consistent with the observation of a transient green-blue intermediate in the reaction between Cp*Ni(acac) and LiNH(*p*-tol). In an attempt to observe monomeric Cp*NiNH(*p*-tol) by low-temperature NMR spectroscopy, the reaction was performed in an NMR tube using THF-d_8. However, NMR analysis at −50 °C was complicated by the paramagnetic starting material and the poorly-soluble lithium salts, and the only identifiable amidonickel complex was **1**.

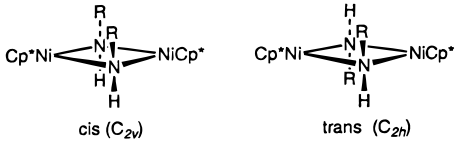

Figure 1. Geometric isomers of $[Cp^*Ni(\mu\text{-}NHR)]_2$.

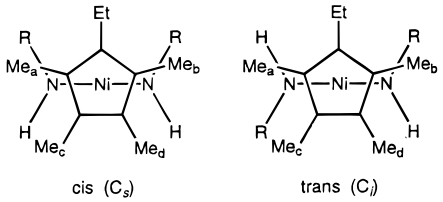

Figure 2. Isomers of $[Cp^{Et}Ni(\mu\text{-}NHR)]_2$, viewed down the Ni−Ni axis.

Nevertheless, it was possible to obtain evidence supporting the intermediacy of the monomer with a low-temperature trapping experiment. Addition of trimethylphosphine to the green-blue solution at −78 °C immediately gave a blue solution of $Cp^*Ni(PMe_3)(NH(p\text{-tol}))$ (**5**). Reaction of the dimer **1** with PMe_3 gives **5** only after several hours at room temperature (*vide infra*), so this low-temperature reaction cannot be preceded by dimerization. Hence, it appears that PMe_3 is trapping monomeric $Cp^*Ni(NH(p\text{-tol}))$ that persists under the reaction conditions at low temperature. Attempted trapping by pyridine did not hinder the formation of dimer, although the presence of pyridine made the reaction proceed cleanly at a higher temperature. The syntheses of **1** and **2** described in the Experimental Section demonstrate both methods for making these arylamido dimers.

Solution Structural Characterization. Mass spectrometry indicated that these nickel amides were dimers in the gas phase; we also desired confirmation that the dimeric structures persist in solution and in the solid state. Both solution NMR techniques and X-ray crystal structure analysis proved useful in this effort.

An $M_2(\mu\text{-}NHR)_2$ skeleton allows the presence of two geometric isomers, cis and trans, that have idealized C_{2v} and C_{2h} symmetries, respectively (Figure 1). In the case of **4**, only one isomer was observed, but for **1**, **2**, and **3**, mixtures of isomers were generally obtained. It was not possible to separate these isomers by crystallization, but cis and trans isomers could be distinguished in solution by their different ^1H NMR spectra. The cis and trans isomers of **1**−**4** are expected to have the same number of resonances in their NMR spectra, so there was no definitive way to determine which isomer corresponded to each set of resonances. However, the lower symmetry of the Cp^{Et} ligand allowed us to distinguish cis (C_s symmetry) from trans (C_i symmetry) isomers in **1′**, **3′**, and **4′** (Figure 2). In the cis (C_s) isomers, methyl groups a and b are rendered chemically equivalent by the molecular mirror plane, as are methyl groups c and d, so two singlets are expected in the proton and carbon NMR spectra, corresponding to Cp^{Et} methyl groups. However, in the trans (C_i) isomers, there are no mirror planes, so all four methyl groups are chemically inequivalent and four different resonances are expected for configurationally stable dimers. The resonances attributable to the amido ligands in **1′**, **3′**, and **4′** were observed at virtually the same chemical shifts as in the Cp* analogues, so it is possible to assign the resonances in the ^1H NMR spectra of **1**−**4** to the appropriate isomers. This

(13) For an extremely unstable nickel alkoxide complex, see: Baranwal, B. P.; Mehrotra, R. C. *Aust. J. Chem.* **1980**, *33*, 37.

(14) No N−H stretching bands were observed in the IR spectra of **1** and **3**, and only weak resonances appeared in the IR spectra of the other dimeric amides. These bands are often weak in metal amides, see: Chisholm, M. H.; Rothwell, I. P. In *Comprehensive Coordination Chemistry*; Wilkinson, G., Ed.; Pergamon: Oxford, 1987; Vol. 2, p 161.

(15) Johnson, C. K., Report ORNL-3794, Oak Ridge National Laboratory, Oak Ridge, TN, 1965.

analysis shows that the predominant isomers formed in the syntheses of **1**−**3** were the trans isomers, but the cis isomer was the exclusive product in the preparation of **4**. The same preference for the cis isomer has been observed in a (*μ-tert*-butylamido)iridium dimer.[6n] (The observation of two distinct isomers for **1**−**3** at temperatures up to 90 °C also shows that the amido ligands of **1**−**3** do not rotate on the NMR time scale.) The crystallographic studies described below provide a basis for rationalizing the observed isomeric distributions.

Another piece of evidence supporting a dimeric structure for **1**−**3** in solution is the observation of variable-temperature ^{1}H NMR data consistent with restricted rotation about the N−C bonds. Dimers **1** and **2** had broad aryl resonances in their proton NMR spectra at room temperature; these coalesced upon warming to 90 °C to two doublets (for **1**) or a doublet and two multiplets (for **2**) for each isomer, and decoalesced to complicated patterns upon cooling to −75 °C. However, heating a sample of **3** to 100 °C in toluene-d_8 did not result in coalescence of any resonances. This variable-temperature behavior is consistent with an aryl group "sandwiched" between Cp* ligands that make it difficult for the aryl groups to rotate out of the plane parallel to the Cp* rings. Since **3** has large *o*-methyl groups, it cannot rotate within the confines of the Cp* rings.

Since several of the above phenomena (observation of multiple isomers and hindered rotation about the N−C bonds) applied only to the arylamides, we desired confirmation that the alkylamide **4** also exists as a dimer in solution. This was accomplished by performing a reaction analogous to the one used to synthesize **4**, but using a 1:1 mixture of LiNH^{t}Bu and LiNH^{t}Amyl (^{t}Amyl = CMe$_2$Et). After workup, the product had a ^{1}H NMR spectrum consistent with a mixture of *three* different nickel amides. The resonances for two of these corresponded to the independently synthesized compounds [Cp*Ni(*μ*-NH^{t}Bu)]$_2$ (**4**) and [Cp*Ni(*μ*-NH^{t}Amyl)]$_2$: the third had resonances in similar positions, consistent with the mixed dimer Cp*Ni(*μ*-NH^{t}Bu)(*μ*-NH^{t}Amyl)NiCp*. These three complexes were produced in the statistically expected ratio of 1:1:2. Incorporation of both amide ligands into one molecule indicates that **4** is a dimer in solution. Thus, **1**−**4** are all dimers, even in the solution phase.

X-ray Crystal Structures of *cis*-1′, *trans*-3′, and 4′. To date, it has not been possible to grow reasonably-sized single crystals of **1**−**4**. However, by using the Cp^{Et} ligand, it was possible to grow crystals of **1′**, **3′**, and **4′** that were suitable for X-ray structural characterization. In each case, data collection (at low temperature) and refinement proceeded without problems; the refinements converged with residuals of 4.2%, 5.4%, and 2.9%, respectively (R_w = 5.2, 6.3, 4.3%). Data collection for **3′** was hampered somewhat by the thinness of the crystals (0.08 mm), but we were able to obtain a satisfactory structure determination using a CCD area detector system through judicious choice of crystal, a higher power setting, and a large semiempirical absorption correction (T_{min}/T_{max} = 0.45).

The structures of **1′**, **3′**, and **4′** are shown as ORTEP[15] diagrams in Figures 3−5. Selected intramolecular distances and angles are in Tables 1−3. In the cases of both **1′** and **4′**, the single crystals were exclusively the cis isomers, and they crystallized in the monoclinic space group *C*2/*c*. In each of these structures, the asymmetric unit consists of only one Cp^{Et}NiNHR unit; the other half of the molecule is related by a crystallographic 2-fold rotation axis normal to the Ni_2N_2 plane. In the case of **3′**, the single crystal contained the trans isomer, and the dimer was found to lie on a crystallographic inversion center in space group $P\bar{1}$. Again, each half of the molecule is crystallographically equivalent, and in this case the inversion

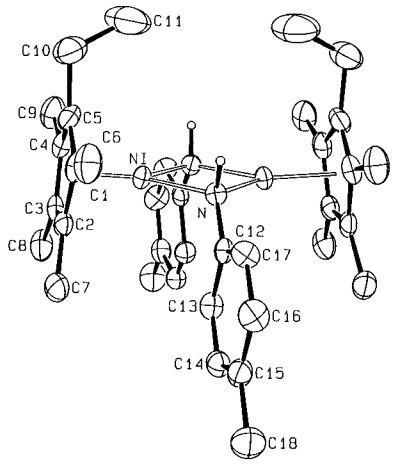

Figure 3. ORTEP diagram of *cis*-**1′**, using 50% probability ellipsoids (except the N-bound H atom, which has arbitrary size). Carbon-bound hydrogen atoms have been omitted for clarity.

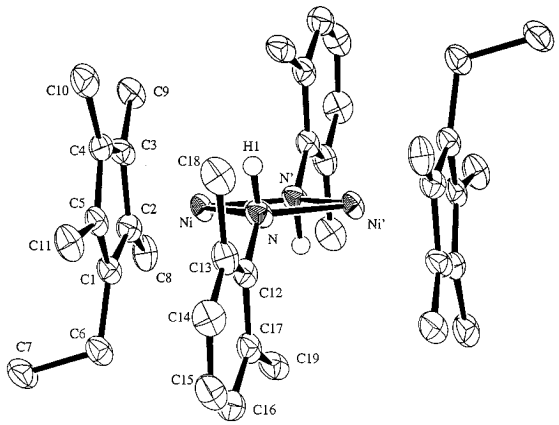

Figure 4. ORTEP diagram of *trans*-**3′**, using 50% probability ellipsoids. Carbon-bound hydrogen atoms have been omitted for clarity.

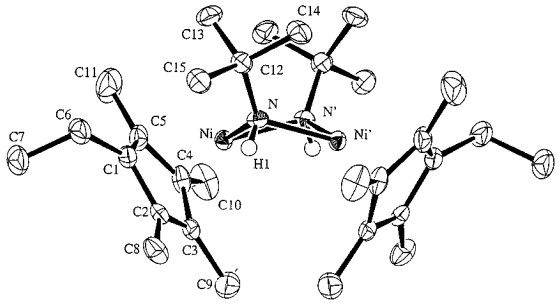

Figure 5. ORTEP diagram of **4′**, using 50% probability ellipsoids. Carbon-bound hydrogen atoms have been omitted for clarity.

center enforces planarity of the Ni_2N_2 ring. No unusually close intermolecular contacts were observed in any of the structures.

The Ni−N bonds in *cis*-**1′** (1.951(3), 1.950(3) Å), *trans*-**3′** (1.957(5), 1.962(6) Å), and **4′** (1.944(2), 1.942(2) Å) are symmetric and longer than those in the only other structurally characterized complex with a simple $Ni_2(amide)_2$ core, the homoleptic dimer [(Ph$_2$N)Ni(*μ*-NPh$_2$)]$_2$, where Ni−N(bridge) distances ranged from 1.90 to 1.92 Å.[6k] This contrast is indicative of a weaker Ni−N interaction in our system, presumably because of the electron-donating power of the cyclopentadienyl ligand relative to the terminal amide ligand.

The most striking difference between the structures of *cis*-**1′**, *trans*-**3′**, and **4′** is that the Ni_2N_2 core is planar in *cis*-**1′** and *trans*-**3′** (*cis*-**1′**, mean distance from the least-squares plane = 0.014 Å; *trans*-**3′**, crystallographically required to be planar), but it is significantly puckered (mean distance from the least-

Table 1. Selected Intramolecular Distances (Å) and Angles (deg) in *cis*-**1′** [a]

Ni−N	1.951(3)	N−Ni−N′	87.7(1)
Ni−N′	1.950(3)	Ni−N−Ni′	92.3(1)
Ni−C(1)	2.085(4)	Cp−Ni−N	135.6
Ni−C(2)	2.165(4)	Cp−Ni−N′	136.6
Ni−C(3)	2.170(4)		
Ni−C(4)	2.088(4)	Ni−N−C(12)	120.4(3)
Ni−C(5)	2.161(4)	Ni′−N−C(12)	119.9(3)
Ni−Cp	1.76		
Ni−Ni′	2.813(1)	C(1)−C(2)−C(3)	107.6(4)
		C(2)−C(3)−C(4)	107.1(4)
N−C(12)	1.410(5)	C(3)−C(4)−C(5)	109.4(4)
		C(4)−C(5)−C(1)	106.2(4)
C(1)−C(2)	1.461(7)	C(5)−C(1)−C(2)	109.0(4)
C(2)−C(3)	1.393(6)		
C(3)−C(4)	1.450(7)		
C(4)−C(5)	1.422(6)		
C(1)−C(5)	1.408(6)		

[a] "Cp" refers to the centroid of the five cyclopentadienyl carbon atoms.

Table 2. Selected Intramolecular Distances (Å) and Angles (deg) in *trans*-**3′** [a]

Ni−N	1.957(5)	N−Ni−N′	85.4(2)
Ni−N′	1.962(6)	Ni−N−Ni′	94.6(2)
Ni−C(1)	2.146(6)	Cp−Ni−N	137.1
Ni−C(2)	2.115(6)	Cp−Ni−N′	137.4
Ni−C(3)	2.197(6)		
Ni−C(4)	2.208(7)	Ni−N−C(12)	119.9(4)
Ni−C(5)	2.093(7)	Ni′−N−C(12)	121.0(4)
Ni−Cp	1.78		
Ni−Ni′	2.880(1)	C(1)−C(2)−C(3)	108.4(5)
		C(2)−C(3)−C(4)	107.9(4)
N−C(12)	1.426(7)	C(3)−C(4)−C(5)	107.6(4)
N−H(N)	0.99(5)	C(1)−C(5)−C(4)	108.5(4)
		C(2)−C(1)−C(5)	107.0(4)
C(1)−C(2)	1.395(7)		
C(2)−C(3)	1.478(7)		
C(3)−C(4)	1.384(8)		
C(4)−C(5)	1.453(7)		
C(1)−C(5)	1.437(7)		

[a] "Cp" refers to the centroid of the five cyclopentadienyl carbon atoms.

Table 3. Selected Intramolecular Distances (Å) and Angles (deg) in **4′** [a]

Ni−N	1.944(2)	N−Ni−N′	85.50(9)
Ni−N′	1.942(2)	Ni−N−Ni′	88.16(8)
Ni−C(1)	2.155(2)	Cp−Ni−N	135.9
Ni−C(2)	2.173(2)	Cp−Ni−N′	135.2
Ni−C(3)	2.198(2)		
Ni−C(4)	2.104(2)	Ni−N−C(12)	124.7(1)
Ni−C(5)	2.192(3)	Ni′−N−C(12)	126.7(1)
Ni−Cp	1.79		
Ni− Ni′	2.7029(5)	C(1)−C(2)−C(3)	108.6(2)
		C(2)−C(3)−C(4)	106.5(2)
N−C(12)	1.500(3)	C(3)−C(4)−C(5)	109.6(2)
N−H(N)	0.80(3)	C(4)−C(5)−C(1)	106.6(2)
		C(5)−C(1)−C(2)	108.3(2)
C(1)−C(2)	1.457(3)		
C(2)−C(3)	1.392(3)		
C(3)−C(4)	1.438(3)		
C(4)−C(5)	1.426(4)		
C(1)−C(5)	1.401(3)		

[a] "Cp" refers to the centroid of the five cyclopentadienyl carbon atoms.

squares plane = 0.229 Å) in **4′**. The puckered conformation of **4′** is enforced by the sterically bulky *tert*-butyl groups because they cannot fit as easily between parallel Cp^{Et} ligands as the flat aryl groups in **1′** and **3′** can. To relieve strain, they "push" the Cp^{Et} ligands toward each other and gain more room on one side of the Ni_2N_2 ring. Thus, only the cis isomers of **4** and **4′** are observed because only the cis isomers can accommodate the large, nonplanar ligands.

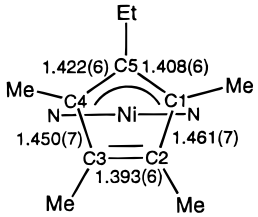

Figure 6. The "ene-allyl" distortion in *cis*-**1′**. Distances are in angstroms (Å).

In the crystal structure of *cis*-**1′**, there are clear signs of an "ene-allyl" distortion of the cyclopentadienyl rings; this is depicted in Figure 6. The C(4)−C(5) and C(5)−C(1) bonds are nearly equivalent and short, as is the C(2)−C(3) bond; these correspond to the "allyl" and "ene" portions of the ring, respectively. This geometry is similar to those observed in the crystal structures of $[CpNi]_2$(biallyl)[16] and Cp*Ni(acac),[12] where this type of distortion was explained by a significant energy difference between the "in-plane" and "out-of-plane" CpM fragment orbitals in the $CpML_2$ system. However, an "ene-allyl" distortion is *not* observed in the crystal structures of *trans*-**3′** and **4′**. Although there are significant distortions from ideal 5-fold symmetry in the cyclopentadienyl rings of both *trans*-**3′** and **4′**, they are distorted in a "diene-yl" fashion, with two short and three long C−C bonds. It is possible that the steric strain from the large amido ligands keeps **3′** and **4′** from "slipping" into a more electronically favorable "ene−allyl" conformation.

The hydrogen atoms in the structures of *trans*-**3′** and **4′** were located, and this allowed us to examine the geometry of the nitrogen-bound hydrogen atoms in **4′** whose resonances lie unusually far upfield in its ^{1}H NMR spectrum (*vide infra*). In both *trans*-**3′** and **4′**, the NH hydrogen atoms lie in the plane defined by the nitrogen atoms and the nitrogen-bound carbons, and there is no sign that the hydrogen atoms "lean" toward either nickel atom. There is a relatively close contact between the NH hydrogen and the nickel atom (2.3 Å) in **4′**, but this appears to be induced by steric forces, not by any direct nickel−hydrogen interaction.

The Ni−Ni distances in *cis*-**1′**, *trans*-**3′**, and **4′** (2.813(1), 2.880(1), and 2.7029(5) Å) do not suggest any Ni−Ni bonding, as opposed to Power's amide dimer, where a Ni−Ni separation of 2.327(2) Å indicated the presence of a metal−metal bond.[6k] Rather, these distances reflect the size of the organic ligand that is trapped between the Cp^{Et} ligands.

Spectroscopy. The most striking spectroscopic characteristic of complexes **1**−**4** is the chemical shifts of the NH protons, which vary from δ 2.59 ppm in the cis isomer of **3** to δ −5.72 ppm in **4** (Table 4). An agostic interaction was immediately suspected as a possible reason for the upfield chemical shifts, but this explanation was discounted by the crystal structure determinations of *trans*-**3′** and **4′** and by the "normal" values of $^1J_{^{15}N-^1H}$ in **1**, **3**, and **4** in solution (Table 4), since an agostic Ni···H−N interaction would be expected to weaken the N−H bond and reduce this coupling constant. Four other potential explanations are as follows: (a) an inductive effect from the basic nitrogen atom, which has been used to explain similar upfield chemical shifts for bridging ligands;[17] (b) ring-current anisotropy from the aromatic cyclopentadienyl rings; (c) an equilibrium between a diamagnetic ground state and a thermally

(16) Smith, A. E. *Inorg. Chem.* **1972**, *11*, 165.

(17) (a) López, G.; Garcia, G.; Ruiz, J.; Sánchez, G.; García, J.; Vicente, C. *J. Chem. Soc., Chem. Commun.* **1989**, 1045. (b) López, G.; Ruiz, J.; García, G.; Vicente, C.; Marti, J. M.; Hermoso, J. A.; Vegas, A.; Martínez-Ripoll, M. *J. Chem. Soc., Dalton Trans.* **1992**, 53.

Table 4. ^{1}H NMR Chemical Shifts and ^{15}N−^{1}H Coupling Constants[a]

	δ_{NH}, ppm	$^1J_{^{15}N-^1H}$, Hz
cis-[Cp*Ni(μ-NHtol)]$_2$ (*cis*-**1**)	−1.79	65
trans-[Cp*Ni(μ-NHtol)]$_2$ (*trans*-**1**)	−2.08	66
cis-[Cp*Ni(μ-NHxyl)]$_2$ (*cis*-**3**)	2.59	
trans-[Cp*Ni(μ-NHxyl)]$_2$ (*trans*-**3**)	−0.11	64
cis-[Cp*Ni(μ-NH^{t}Bu)]$_2$ (**4**)	−5.72	62
Cp*Ni(PMe$_3$)(NHtol) (**5**)	−1.05	68

[a] Coupling constants were measured using natural-abundance samples, using a pulse sequence (details in the Experimental Section) with a double-quantum filter to "remove" resonances from protons attached to ^{14}N. Thus, one observes only resonances from protons attached to ^{15}N ($I = {}^1/_2$), and the result is a doublet, from which the coupling constant can be easily measured.

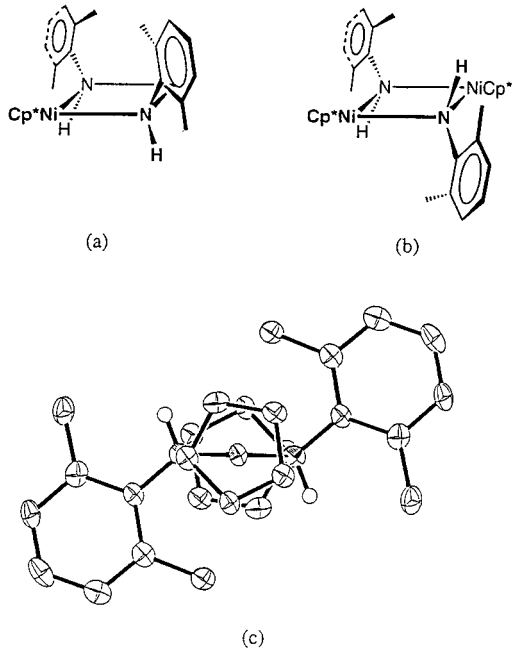

Figure 7. (a, b) Perspective representations of the cis and trans isomers of **3**; (c) view down the Ni−Ni axis in the crystal structure of *trans*-**3′** (cyclopentadienyl substituents have been removed for clarity).

populated electronically excited triplet state, as in Cp*Ni(acac);[12] and (d) an unusually large contact shift from the nickel atom.[18]

An unusual observation in the proton NMR spectrum of **3** is that the xylyl methyl protons resonate at δ 1.75 and 5.39 ppm in the trans isomer and at δ 2.32 and 4.05 ppm in the cis isomer (Figure 7a,b). In attempting to explain both the unusual NH shifts and the unusual xylyl methyl shifts using a single reason, the first and last explanations can be eliminated. Since inductive effects normally travel through bonds, the basicity of the nitrogen atom (explanation (a) in the previous paragraph) would not be able to affect the distant methyl groups. (In addition, the very basic LiNHR compounds do not have NH resonances this far upfield: for example, the N*H* proton in LiNH^{t}Bu resonates at δ −1.50 ppm in THF-d_8.) Likewise, local "paramagnetic" contributions to the chemical shift due to the metal (explanation (d)) would not be able to travel through bonds to the xylyl methyl groups.[18]

There are several pieces of evidence that argue against a spin equilibrium (explanation (c)) in **1**−**4**. The carbon NMR resonances did not occur in unusual positions, and all resonances in the proton and carbon NMR spectra were sharp (except for broadness attributable to the ^{14}N quadrupole). Evans magnetic moment measurements[19] showed that **1′** was diamagnetic within experimental error ($\mu_{eff} < 0.2$), and the chemical shift of the upfield NH resonance in **4** was temperature independent between −80 °C and room temperature. For these reasons, it is unlikely that a spin equilibrium of the type observed in Cp*Ni(acac) is responsible for the unusual NMR spectra.

Thus, it seems most likely that ring-current anisotropy is the source of the unusual chemical shifts observed in **1**−**4**. The unusually high-field NH resonance in **4** can be rationalized through a simple steric argument. Repulsion between the *tert*-butyl groups causes the Ni_2N_2 ring to pucker, as shown in the solid-state structure of **4′** (Figure 5). This causes the NH^{t}Bu groups to rotate about the Ni−Ni axis, bringing the N-bound protons closer to the center of the aromatic cyclopentadienyl ring. Since the effect of the aromatic rings is to shield protons directly above the ring, these protons resonate far upfield. The same effect is undoubtedly present in **1**, **2**, and **3**, but it is apparently complicated by the ring-current anisotropy of the aromatic substituents on the nitrogen atom, and the trends are less simply explained. Ring-current anisotropy can also explain the very different chemical shifts of the xylyl methyl protons in **3**, because the crystal structure of *trans*-**3′** clearly shows that these methyl groups lie at different distances from the cylinder described by the Cp^{Et} rings (Figure 7c). Thus, a combination of inductive effects (which affects the NH protons as in other bridging hydroxides and amides)[17,20] and ring-current anisotropy (which affects the xylyl methyl protons differently) can account for the unusual proton NMR shifts in Table 4.

Isomerization. After purification by crystallization, **1** and **2** were typically obtained as a mixture of trans and cis isomers in a ratio of greater than 10:1, and **3** was obtained with an isomeric ratio of approximately 1:1. (Repeated crystallization gives **3** as exclusively the trans isomer.) However, heating solutions of **1** or **2** converted them to equilibrium mixtures with trans/cis ratios of about 2:1. When **3** was heated, it also isomerized, with the product being exclusively (>98% by ^{1}H NMR spectroscopy) the trans isomer.

In initial attempts to determine the mechanism of these isomerizations by ^{1}H NMR kinetics, we found that heating solutions of **1**−**3** caused significant decomposition. In order to inhibit decomposition, a small amount of Cp_2ZrMe_2 was added to the NMR tube reactions; this has been used successfully in our group as an oxygen and water scavenger.[21] In the presence of the zirconium complex, less than 2% decomposition of the nickel complexes (by integration *vs* an internal standard) was observed over a typical kinetic run at 77 °C for 10 h. In these experiments, a small amount of $Cp_2Zr(Me)(\mu\text{-}O)Zr(Me)Cp_2$ (^{1}H NMR: δ 5.9 ppm), the product of the reaction between Cp_2ZrMe_2 and water,[22] was observed. This shows that the zirconium complex destroyed traces of water on the NMR tube surface and/or in the solvent that had not been removed by conventional drying techniques.

Thus, mixtures of **1**, **2**, or **3**, dimethylzirconocene and ferrocene (as an internal standard) were heated to 76.9 °C in THF-d_8 and monitored by one-pulse proton NMR spectroscopy,

(18) For a discussion of paramagnetic contributions to the chemical shift, see: Drago, R. S. *Physical Methods for Chemists*; Saunders College Publishing: Orlando, 1992; pp 232−243.

(19) (a) Bax, A.; Griffey, R. H.; Hawkins, B. L. *J. Magn. Reson.* **1988**, *55*, 301. (b) Evans, D. F. *J. Chem. Soc.* **1959**, 2003. (c) Baker, M. V.; Field, L. D.; Hambley, T. W. *Inorg. Chem.* **1988**, *27*, 2872. (d) Jolly, W. L. *The Synthesis and Characterization of Inorganic Compounds*; Waveland: Prospect Heights, IL, 1970.

(20) (a) Park, S.; Rheingold, A. L.; Roundhill, D. M. *Organometallics* **1991**, *10*, 615. (b) Blake, R. E.; Heyn, R. H.; Tilley, T. D. *Polyhedron* **1992**, *11*, 709.

(21) (a) Proulx, G.; Bergman, R. G. *J. Am. Chem. Soc.* **1995**, *117*, 6382. (b) Hanna, T. A.; Baranger, A. M.; Walsh, P. J.; Bergman, R. G. *J. Am. Chem. Soc.* **1995**, *117*, 3292.

(22) Marsella, J. A.; Folting, K.; Huffman, J. C.; Caulton, K. G. *J. Am. Chem. Soc.* **1981**, *103*, 5596.

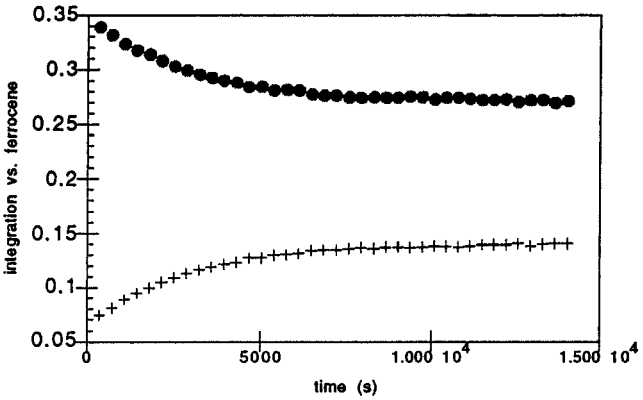

Figure 8. Plot of [*cis*-**1**] (+) and [*trans*-**1**] (●) *vs* time at 76.9 °C.

Table 5. Rate Constants Calculated from Kinetic Runs in THF-d_8 at 76.9 °C

	k_{obs}/ 10^{-4} s^{-1}	K_{eq}	k_1/ 10^{-4} s^{-1}	k_{-1}/ 10^{-4} s^{-1}
[Cp*Ni(μ-NHtol)]$_2$ (**1**)	3.5 ± 0.3	2.3 ± 0.3	2.4	1.1
[Cp*Ni(μ-NHPh)]$_2$ (**2**)	5.5 ± 0.5	2.4 ± 0.3	3.9	1.6
[Cp*Ni(μ-NHxyl)]$_2$ (**3**)	0.34 ± 0.04	>50	0.34	

with data points taken every 6 min. Some of the peaks for cis and trans isomers overlapped, but when peaks which did not overlap were monitored, good first-order time dependence curves were obtained. There were no signs of reaction of Cp_2ZrMe_2 with the nickel complexes or with the ferrocene. Repeating the isomerization of *trans*-**2** without Cp_2ZrMe_2 present gave an identical isomerization rate, but as stated earlier, this was accompanied by decomposition of the nickel complexes.

A typical plot of [*cis*-**1**] and [*trans*-**1**] *vs* time is shown in Figure 8. The isomerizations of **1**−**3** were found to be first order to approximately 5 half-lives.[23] The first-order rate constants (k_{obs}) for these processes are displayed in Table 5. In the cases of **1** and **2**, values for K_{eq} estimated from ^{1}H NMR data allow us to derive k_1 and k_{-1} from k_{obs} as shown in eq 1. In the case of **3**, since the equilibrium lies completely on the side of the trans isomer, one can make the approximation $k_1 \approx k_{obs}$.

$$\text{cis} \underset{k_{-1}}{\overset{k_1}{\rightleftharpoons}} \text{trans} \qquad K_{eq} = k_1/k_{-1};\ k_{obs} = k_1 + k_{-1} \qquad (1)$$

Few studies have been done on the isomerization of dimers like **1**−**3**. Several groups have looked at dimers [$R_2Al(\mu$-$NHR)]_2$ and their isomerization and conversion to trimers and imides.[24] Mechanistic studies of these reactions indicated that this isomerization proceeds through a ring-opened Lewis base adduct.[24e] One group has proposed a π-cycloreversion/cycloaddition mechanism for this process, but their data do not support that conclusion.[25] Mays and co-workers have studied the isomerization of [$(CO)_4Mn(\mu$-$PHPh)]_2$; their study indicates that this proceeds through a mechanism where one Mn−P bond is broken, but the isomerization can also take place through a deprotonation/reprotonation mechanism in the presence of a strong base (^{n}BuLi).[26] Two series of palladium amide dimers with $M_2(NHR)_2$ cores have been isolated; in one case, no exchange between isomers occurred at high temperature,[6e] and in the other, isomerization took place at room temperature, but the process involved several isomers that could not be unequivocally identified.[6g]

The data allow us to distinguish the mechanisms shown in Scheme 2. Pathway (a), which is dissociative in nature, is ruled out because only a small amount (<5%) of crossover (*vide infra*) occurred between **1** and **2** when they were heated together under the conditions used for the kinetic runs. Associative mechanisms like (d) are not satisfactory because plots of log $|[A] - [A]_{eq}|$ vs time were linear, and the observed first-order rate constant did not change upon doubling the concentration of nickel complex. Moreover, when the isomerization of **1** was performed in toluene-d_8 instead of THF-d_8, k_{obs} was 3.7 ± 0.4 × 10^{-4} s^{-1}. Since the coordination ability of the solvent did not affect the rate constant, it is unlikely that the rate-determining step involves any significant interaction with solvent as in (c). Thus, the mechanism most consistent with the data is (b), in which the isomerization proceeds by one dative bond breaking followed by the amido ligand rotating; rapid inversion at the three-coordinate nitrogen then allows the amido ligand to bind with the opposite orientation. We have not been able to identify a trapping agent that is capable of diverting the presumed ring-opened intermediate into a stable product.

The values of k_1 for the isomerizations of **1**−**3** (Table 5) parallel the coalescence temperatures for the aryl protons in their ^{1}H NMR spectra (*vide supra*): the tolyl and phenyl groups in **1** and **2** can rotate with a relatively low barrier, while the 2,6-xylyl group in **3** does not rotate. This suggests that the rate-determining step in the isomerization process is the rotation of the amido ligand, because the sterically hindered 2,6-xylylamido complex **3** isomerizes an order of magnitude more slowly than **1** and **2**. The observation of a slower rate with larger ligands further refutes dissociative mechanisms (including mechanism (a)) for the isomerization.

Minimal crossover occurred in thermolyses (77 °C for 10 h) of **1**−**3** in the presence of dimethylzirconocene, in C_6D_6 or THF-d_8 solutions, as mentioned earlier. However, a mixture of **1** and **2** in C_6D_6 solution was converted to the mixed amido complex Cp*Ni(μ-NH(*p*-tol))(μ-NHPh)NiCp* over several weeks at 45 °C (eq 2).

$$[\text{Cp*Ni}(\mu\text{-NH}(p\text{-tol}))]_2\ (\mathbf{1}) + [\text{Cp*Ni}(\mu\text{-NHPh})]_2\ (\mathbf{2}) \rightleftharpoons \text{Cp*Ni}(\mu\text{-NH}(p\text{-tol}))(\mu\text{-NHPh})\text{NiCp*} \qquad (2)$$

This process was slowed, but not totally inhibited, by the addition of Cp_2ZrMe_2, implying that it occurs concurrently *via* water-catalyzed and -uncatalyzed mechanisms. The proton NMR resonances for the mixed amido complex lie very close to the resonances for **1** and **2**, and the characteristic singlets for the Cp* protons in both isomers of all three compounds can be distinguished in C_6D_6 solution. The appearance of a new envelope at *m/z* 584 in the mass spectrum of the product (Figure 9) is consistent with our formulation of this product.

(23) The isomerization of **3** was too slow at 76.9 °C to follow for more than 1 half-life, so this isomerization was repeated at 97.6 °C; we observed first-order behavior to 5 half-lives, with a rate constant of $k_{obs} = 5.5 \pm 0.4 \times 10^{-4}$ s^{-1}.

(24) (a) Bowen, R. E.; Gosling, K. *J. Chem. Soc., Dalton Trans.* **1974**, 964. (b) Wakatsuki, K.; Tanaka, T. *Bull. Chem. Soc. Jpn.* **1975**, *48*, 1475. (c) Al-Wassil, A.-A. I.; Hitchcock, P. B.; Sarisaban, S.; Smith, J. D.; Wilson, C. L. *J. Chem. Soc., Dalton Trans.* **1985**, 1929. (d) Sauls, F. C.; Czekaj, C. L.; Interrante, L. V. *Inorg. Chem.* **1990**, *29*, 4688. (e) Choquette, D. M.; Trimm, M. J.; Hobbs, J. L.; Rahim, M. M.; Ahmed, K. J.; Planalp, R. P. *Organometallics* **1992**, *11*, 529.

(25) Beachley observed an equilibrium ratio of *ca.* 5:1 for *cis*- and *trans*-$[Me_2AlN(Me)(Ph)]_2$, and rationalized the predominance of the cis isomer on the basis of a transition-state argument involving cycloadditions. However, we were somewhat puzzled by this discussion, because near the end of ref 25b the authors make clear that the observed cis/trans ratios are thermodynamically controlled. See: (a) Beachley, O. T.; Tessier-Youngs, C. *Inorg. Chem.* **1979**, *18*, 3188. (b) Beachley, O. T.; Bueno, C.; Churchill, M. R.; Hallock, R. B.; Simmons, R. G. *Inorg. Chem.* **1981**, *20*, 2423.

(26) Brown, M. P.; Buckett, J.; Harding, M. M.; Lynden-Bell, R. M.; Mays, M. J.; Woulfe, K. W. *J. Chem. Soc., Dalton Trans.* **1991**, 3097. They saw faster isomerization rates in polar solvents; this implicates a mechanism with solvent coordination, as in (c).

Scheme 2

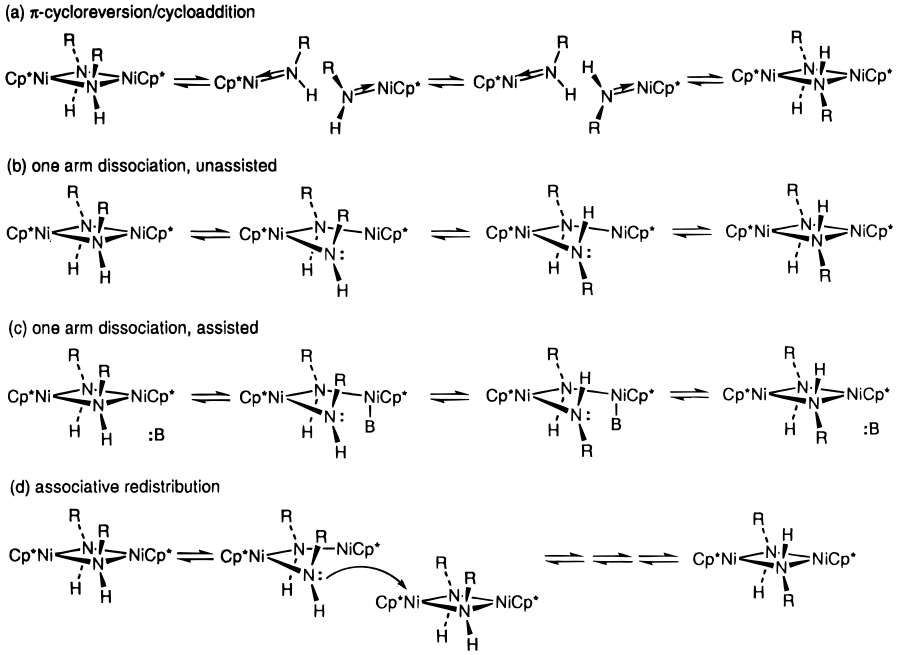

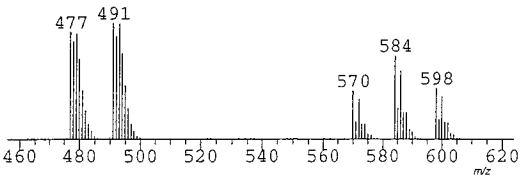

Figure 9. A portion of the electron-impact mass spectrum of the product obtained by heating a mixture of **1** (M^+, *m/z* 598) and **2** (M^+, *m/z* 570) at 45 °C for 2 weeks. The envelopes on the left are assigned as the fragments $[Cp^*Ni]_2(\mu\text{-NHPh})^+$ and $[Cp^*Ni]_2(\mu\text{-NHtol})^+$, respectively.

Scheme 3

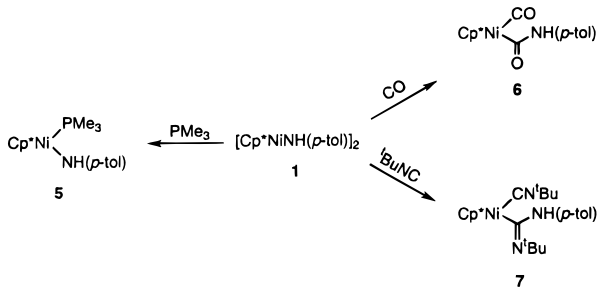

These mixed amides can also be formed by reaction of Cp*Ni(acac) with a mixture of lithium amides using procedures analogous to those in Scheme 1; using this methodology, we have also prepared Cp*Ni(μ-NH^{t}Bu)(μ-NH^{t}Amyl)NiCp* (^{t}Amyl = CMe_2Et) (*vide supra*) and Cp*Ni(μ-NH(*p*-tol))(μ-NHxyl)-NiCp*. However, the materials isolated from these reactions were inseparable mixtures of the symmetrically substituted dimers and the mixed products.[27] The *tert*-butylamido/*tert*-amylamido and *p*-tolylamido/2,6-xylylamido mixed dimers are notable in that they *cannot* be formed by "crossover" reactions analogous to eq 2; heating a mixture of **1** and **3**, for example, gives only decomposition. The higher reactivity of **1** (with respect to the bulkier complexes **3** and **4**) in crossover reactions parallels its reactivity toward small molecules, which will be presented in the following section.

Reactions of 1 with Small Molecules. We hoped to replace the dative Ni−N bond in these dimers with a strongly coordinating neutral Lewis base such as carbon monoxide, isonitrile, or phosphine, to give monomeric complexes Cp*Ni-(L)(NHR). However, this strategy was not successful for complexes **3** or **4**; when treated with 2 equiv of PMe_3, each slowly gave $Ni(PMe_3)_4$ as the only identifiable nickel-containing product. Similarly, reaction of **3** or **4** with *tert*-butyl isonitrile slowly gave $Ni(CN^tBu)_4$. We were not able to determine the fate of the amido ligand or the Cp* ligand in these reactions, although amine was generally observed as a byproduct (by ^{1}H NMR spectroscopy). When carbon monoxide (1 atm) was added to **4**, the solution turned red over the course of several days. As this is the same time scale as that associated with decomposition of **4**, the reaction was repeated at higher pressure. Under 15 atm of CO, the solution rapidly turned red, but the starting material and $[Cp^*Ni(\mu\text{-CO})]_2$[28] were again the only identified nickel-containing products. We also identified the urea, $(^tBuNH)_2C{=}O$, by NMR spectroscopy and by analogy to the product, $((p\text{-tol})NH)_2C{=}O$, identified in an analogous reaction described below. Other Lewis bases such as pyridine and amines did not react with **3** or **4** prior to decomposition. Thus, it has not been possible to cleave these dimers while maintaining the nickel−nitrogen bond; this is consistent with the inaccessibility of the Ni_2N_2 core that is evident in the crystal structures of *trans*-**3′** and **4′**.

Dimer **1**, on the other hand, was easily cleaved by CO, ^{t}BuNC, or PMe_3 to give monomeric products (Scheme 3). When a solution of **1** in toluene was stirred under an atmosphere of carbon monoxide for 12 h, a red solution resulted which contained both the known red compound, $[Cp^*Ni(\mu\text{-CO})]_2$,[28] and the new nickel carboxamide complex Cp*Ni(CO)(C(O)-NH(*p*-tol)) (**6**). Dilute reaction conditions and lowered temperature maximized the amount of **6** in this mixture. At *ca.* 0.5 mM concentration of **1** and 0 °C, we obtained $[Cp^*Ni(\mu\text{-CO})]_2$ and **6** in a 3:2 ratio and isolated **6** in 39% yield as an orange powder after removal of volatile materials and washing with hexamethyldisiloxane to remove $[Cp^*Ni(\mu\text{-CO})]_2$.

(27) Cp*Ni(μ-NH^{t}Bu)(μ-NH^{t}Amyl)NiCp* was obtained in a roughly statistical ratio of products, as mentioned above. Cp*Ni(μ-NH(*p*-tol))(μ-NHxyl)NiCp* could be separated from **1** by crystallization, but we were unable to separate the two isomers of the mixed product from the two isomers of **3**.

(28) Mise, T.; Yamazaki, H. *J. Organomet. Chem.* **1979**, *164*, 391.

Samples of **6** were stable in solution at room temperature for short periods of time, but decomposed within hours in the solid state or in solution at room temperature. This thermal instability precluded mass spectrometric characterization, but elemental analysis and ^{1}H NMR spectroscopy were consistent with our formulation of this product. The infrared spectrum of **6** displays absorptions at 2015 and 1647 cm^{-1}, indicating the presence of C≡O and C═O bonds, respectively. When the reaction was repeated using ^{13}CO, *two* resonances were observed in the ^{13}C{^{1}H} NMR spectrum, a doublet ($^2J_{CC}$ = 9 Hz) at δ 192.4 ppm and a broad resonance at δ 185.2 ppm. These are consistent with the nickel-bound carbons of a terminal carbonyl ligand and of a carboxamide ligand, coupled to each other (the resonance of the latter is broadened by the ^{14}N quadrupole). When a C_6D_6 solution of **6** was allowed to stand at ambient temperature for 2 days, it decomposed to a red solution and a white powder: the supernatant solution consisted of [Cp*Ni(μ-CO)]$_2$ (greater than 90% purity by ^{1}H NMR spectroscopy), and the urea ((*p*-tol)NH)$_2$C═O was the major component of the powder.

The reaction of **1** with *tert*-butyl isonitrile gave the analogous amidinylnickel complex Cp*Ni(CN^{t}Bu)(C(N^{t}Bu)NH(*p*-tol)) (**7**), which was isolated as a brown solid in 63% yield. This product was much more stable than its carbonyl analogue. The proton NMR spectrum of **7** contains *tert*-butyl resonances at δ 0.92 and 1.57 ppm, and the IR spectrum displays absorptions for C≡N and C═N at 2120 and 1557 cm^{-1}, respectively. It was possible to characterize **7** by mass spectrometry and elemental analysis, and each of these confirmed our description of this complex as an insertion product analogous to **6**. Alkenes and alkynes did not insert into the nickel−nitrogen bond of **1**.

The new ligands in **6** and **7** are interesting in that they are the hypothetical products from the protonation of a coordinated isocyanate or carbodiimide, respectively. Such a route has been employed in synthesizing vanadium and cobalt complexes containing amidinyl ligands.[29] Even more interesting is viewing the amidinyl ligand in **7** as a deprotonated diaminocarbene complex. A platinum amidinyl complex has recently been synthesized using this method.[30] The insertion of an isocyanide into a metal−nitrogen bond as described here is a complementary entry into this ligand system.

Insertion into the M−N bond in amido complexes is uncommon but not unprecedented for late-transition-metal amides.[1b] In some recent studies, it is difficult to determine whether CO inserts into an M−N bond or an M−C bond because the insertion is immediately followed by reductive elimination.[8a,31] It is often assumed that the carbonyl group inserts into the M−C bond, despite examples of complexes in which M−N insertion is preferred over M−C insertion.[1a] In the reactions described here, though, it is clear that CO and ^{t}BuNC insertion into the Ni−N bond of **1** is facile. The most reasonable mechanism involves cleavage of the dimer to give Cp*Ni(L)(NH(*p*-tol)) (L = CO, ^{t}BuNC) as an intermediate, followed by migratory insertion and coordination of another molecule of CO or ^{t}BuNC. While it is interesting that cleavage of the M_2N_2 core is possible, we desired a method of cleavage that would retain the nickel−nitrogen bond.

In the presence of 2 equiv of PMe_3, **1** was converted to a blue solution that was judged by proton NMR spectroscopy to contain only (>95%) the desired monomer Cp*Ni(PMe_3)(NH(*p*-tol)) (**5**) after 10 h at room temperature. Unfortunately, it proved impossible to isolate this complex, because it decomposed to mixtures of **1** and Ni(PMe_3)$_4$ upon standing in solution or exposure to vacuum. Addition of excess PMe_3 resulted in formation of Ni(PMe_3)$_4$. In the proton NMR spectrum of **5**, an upfield resonance (δ −1.05 ppm) was observed; its assignment as the NH proton was confirmed by observation of $^1J_{^{15}N-^1H}$ = 68 Hz in a ^{15}N-filtered proton NMR spectrum (Table 4). Coordination of the phosphine ligand was evident from phosphorus coupling to the Cp* ligand (J = 1.6 Hz) and a new resonance in the ^{31}P{^{1}H} NMR at δ −5.9 ppm.

The reaction of **1** with PMe_3 occurred much more quickly than the cis/trans isomerization described earlier. It is possible that the reaction with PMe_3 proceeds through the ring-opened intermediate that eventually leads to cis/trans isomerization. However, the data do not rule out the intermediacy of an associative intermediate such as Cp*Ni(PMe_3)(μ-NH(*p*-tol))$_2$NiCp*. Twenty-electron Cp*Ni complexes have been isolated and crystallographically characterized as such,[12] and they are not unreasonable intermediates in this process if steric hindrance is not excessive. Ring slippage is also a possibility in transition-metal cyclopentadienyl complexes. The instability of **5** in solution and its intolerance to added phosphine have prevented us from performing mechanistic studies to resolve this question.

We have also found that arylamines exchange with the amide ligands in **1** and **2**. Thus, reaction of **1** with a large excess of aniline at 45 °C slowly gave mixtures of **1**, **2**, and Cp*Ni(μ-NH(*p*-tol))(μ-NHPh)NiCp*, until eventually the solution contained almost exclusively **2**. Other Brønsted acids such as water and *p*-cresol reacted with **1**, but did so slowly and/or not cleanly. We have not been able to characterize the products of these reactions, but they were clearly paramagnetic, giving ^{1}H NMR spectra with broad resonances at unusual chemical shifts (for example, the product of **1** and H_2O gives one broad resonance at δ 196 ppm in C_6D_6!). It is likely that these products are polynuclear clusters.

Finally, we have attempted several routes for removing the hydrogen atom from the nitrogen in the amide ligand to give an imido complex. None of the reagents we have tried (MeLi, KO^{t}Bu, Ph_3CBF_4, ^{t}BuONO, (*p*-^{t}BuC_6H_4)$_3$C$^\bullet$ [32]) reacted cleanly with **1** or with **4**.

Conclusions

Although the bulky Cp* ligand might be expected to give monomeric amide products from the reaction conditions in Scheme 1, only dimeric [Cp*Ni(μ-NHR)]$_2$ complexes have been isolated. This indicates that, despite the entropic and steric costs of dimerization, the nitrogen−nickel dative bond provides more stabilization than the hypothetical nickel−nitrogen π bond of a Cp*NiNHR monomer. These Cp*Ni complexes seemingly go to great lengths (including the toleration of severe steric strain in **4′**, as evidenced by its crystal structure) to dimerize in order to avoid coordinative unsaturation at the metal center. However, the strong steric forces produce effects such as unusual chemical shifts in the proton NMR and hindered rotation about the C−N single bonds. We have also presented a striking example of the effects of ring-current anisotropy, which is the best way to explain the abnormally high field at which the N−H protons in these complexes (especially **4**) resonate.

We have also completed a mechanistic study on the cis/trans isomerization of the Ni_2N_2 core of **1**−**3**. The data indicate that this process is initiated by cleavage of a Ni−N dative bond,

(29) (a) Pasquali, M.; Gambarotta, S.; Floriani, C.; Villa, A. C.; Guastini, C. *Inorg. Chem.* **1981**, *20*, 165. (b) Horlin, G.; Mahr, N.; Werner, H. *Organometallics* **1993**, *12*, 1993.

(30) Crociani, B.; DiBianca, F.; Fontana, A.; Forsellini, E.; Bombieri, G. *J. Chem. Soc., Dalton Trans.* **1994**, 407.

(31) Yamamoto, T.; Sano, K.; Osakada, K.; Komiya, S.; Yamamoto, A.; Kushi, Y.; Tada, T. *Organometallics* **1990**, *9*, 2396.

(32) Eisenberg, D. C.; Lawrie, C. J. C.; Moody, A. E.; Norton, J. R. *J. Am. Chem. Soc.* **1991**, *113*, 4888.

followed by rotation of the amido ligand and recoordination. This study showed that the aforementioned steric effects constrain the rotation of the NHR unit, making this the slow step for the process. The mechanism is similar to that observed for aluminum amido dimers;[24e] however, the bulkiness of this nickel system prevents catalysis by Lewis bases.

Finally, we have shown that insertion into the metal−nitrogen bond in **1** by carbon monoxide and *tert*-butyl isonitrile is a facile process, and that phosphines can also effect the cleavage of the dimer. These reactions are inefficient with large amido ligands or with large phosphines, which is almost certainly a result of the steric constraints on these bulky dimeric nickel complexes. However, the fact that **1** will react with Lewis bases stands in contrast to similar complexes of iridium and platinum, in which the M_2N_2 core is unreactive even to fairly stringent conditions.[6e,7b,33] This indicates that the first-row transition metal indeed has higher reactivity, and we expect that this reactivity will eventually be utilized for catalytic applications.

Experimental Section

General. All manipulations were carried out in oven-dried glassware either using standard Schlenk techniques or in a Vacuum Atmospheres circulating inert atmosphere glovebox. Pentane, diethyl ether, hexanes, hexamethyldisiloxane, toluene, toluene-d_8, C_6H_6, C_6D_6, THF, THF-d_8, and PMe_3 were dried over Na/benzophenone. Methylene chloride, acetonitrile, propionitrile, chloroform-*d*, aniline, propionitrile, *tert*-amylamine and *tert*-butylamine were dried over calcium hydride. *p*-Toluidine, ferrocene, and Cp_2ZrMe_2 were sublimed prior to use. *tert*-Butyl isonitrile was dried over 4 Å molecular sieves. Silica gel (Merck, 60 Å, 230−400 mesh, grade 9385) and Celite were dried overnight at 200 °C under dynamic vacuum. Lithium amides were prepared by adding a slight deficiency of *n*-butyllithium or methyllithium (in hexanes or diethyl ether, respectively) to a hexanes or toluene solution of the appropriate amine, washing with hexanes or toluene, and removing volatile materials *in vacuo*. $MgCp^*_2$[34] and $MgCp^{Et}_2$ were prepared by heating Cp*H or $Cp^{Et}H$ and Bu_2Mg (0.85 M in heptane solution, 0.5 equiv) to reflux overnight, crystallized by cooling the heptane solution to −80 °C, and recrystallized from hexanes. Successful synthesis of the new compound $MgCp^{Et}_2$ was verified by the ^{1}H NMR spectrum of the product in C_6D_6 (δ 2.38 (q, J = 7.5 Hz, 2, Et), 1.94 (s, 6, Me), 1.93 (s, 6, Me), 1.01 (t, 3, Et)). $Ni(acac)_2$ and Cp*Ni(acac) were synthesized according to published procedures.[12,35] Cp*Ni(acac) was generally sublimed before use. Carbon monoxide was obtained from Matheson and used as received. All other starting materials were of reagent grade and were purified according to standard procedures, as necessary.[36] Proton NMR spectra were recorded on a Bruker AMX-300 spectrometer (300 MHz) and $^{13}C\{^1H\}$ and $^{31}P\{^1H\}$ NMR spectra were recorded on a Bruker AMX-400 spectrometer (100.6 MHz for carbon, 162.1 MHz for phosphorus). Chemical shifts are reported in parts per million (δ), coupling constants are reported in hertz (Hz) and integrations are reported in number of protons. Unless otherwise indicated, $^{13}C\{^1H\}$ NMR resonances are singlets. Chemical shifts are referenced internally to the C_6D_6 solvent peaks at δ 7.15 (^{1}H) and 128.0 (^{13}C) ppm, the THF-d_8 solvent peaks at δ 3.58 (^{1}H) and 67.4 (^{13}C) ppm, or the $CDCl_3$ solvent peak at δ 7.26 ppm. In some cases, DEPT was used to assign the $^{13}C\{^1H\}$ NMR resonances as CH_3, CH_2, CH, or quaternary. Unless otherwise indicated, NMR spectra were recorded as C_6D_6 solutions. In the ^{1}H NMR spectra of **1**, **2**, **1′**, and **2′**, the broadness of some aryl peaks at room temperature (*vide supra*) prevented accurate integration of these peaks. ^{15}N-filtered ^{1}H NMR spectra were obtained using a pulse sequence similar to that described by Griffey,[19a] modified to give only the one-dimensional ^{1}H NMR spectrum. Effective magnetic moment (μ_{eff}) measurements were made using Evans' method[19b] using C_6D_6 solutions, with the standard formula[19c] and values for diamagnetic corrections.[19d] IR spectra were recorded on a Mattson Galaxy Series FTIR 3000 spectrometer, as Nujol mulls on NaCl plates, as pressed KBr pellets, or as solutions between NaCl plates in a solution cell, and the frequencies are reported in cm^{-1}. Melting points of samples in sealed capillary tubes under N_2 were recorded on a Thomas Hoover melting point apparatus, and are uncorrected. Elemental analyses were performed at the UCB Microanalysis Facility. Mass spectral analyses were performed by the UCB Mass Spectrometry Laboratory on AEI-MS12, Kratos MS-50, or VG ProSpec instruments. Mass spectral results are reported in *m/z* using the most intense peak in each envelope; relative abundances are listed in parentheses. Unless otherwise indicated, the isotopic distribution of the parent ion envelope matched the simulated spectrum.

[Cp*Ni(μ-NH(*p*-tol))]$_2$ (1). A flask was charged with Cp*Ni(acac) (619 mg, 2.11 mmol), LiNH(*p*-tol) (250 mg, 2.21 mmol), and a stir bar and capped with a vacuum adapter. The flask was cooled to −196 °C, THF (60 mL) was condensed into the flask, and the mixture was warmed to −40 °C with stirring. After 30 min, the blue-green solution was allowed to warm to room temperature. After an additional hour of stirring, the volatile materials were removed *in vacuo*, leaving a purple-brown residue. In the glovebox, the residue was extracted into pentane (130 mL); the resulting solution was filtered through a Celite pad (2 × 1 cm) and concentrated to 70 mL. Slow cooling to −80 °C gave a purple powder. Concentration and cooling of the mother liquor gave a second crop for a total yield of 414 mg (65.3%) of **1**. ^{1}H NMR: δ 7.62 (br m, 2, aryl), 6.86 (m, 2, aryl), 2.16 (s, 3, C_6H_4*Me*, trans), 2.11 (s, 3, C_6H_4*Me*, cis), 1.12 (s, 15, C_5Me_5, cis), 1.11 (s, 15, C_5Me_5, trans), −1.79 (s, 1, NH, cis), −2.08 (s, 1, NH, trans). $^{13}C\{^1H\}$ NMR (trans isomer,[37] THF-d_8): δ 157.0 (aryl), 128.7 (aryl), 127.4 (aryl), 124.1 (aryl), 98.1 (C_5Me_5), 20.7 (C_6H_4*Me*), 8.9 (C_5*Me*$_5$). Mp: 199 - 201 °C dec. IR (C_6D_6): 1608 (w), 1502 (s), 1246 (m). EI-MS: 299 (70), 493 (100), 598 (79, M^+). Anal. Calcd for $C_{34}H_{46}Ni_2N_2$: C, 68.04; H, 7.73; N, 4.67. Found: C, 67.86; H, 7.73; N, 4.75.

[Cp*Ni(μ-NHPh)]$_2$ (2). To a three-necked flask charged with Cp*Ni(acac) (277 mg, 0.945 mmol) and fitted with a septum, a stopper, and a gas inlet, pyridine (15 mL) was added *via* cannula. The orange solution was cooled to −40 °C, and a solution of LiNHPh (101 mg, 1.02 mmol) in THF (10 mL), also cooled to −40 °C, was slowly added *via* cannula, and the solution became very dark. The solution was stirred for 1 h at −40 °C, then warmed to room temperature, and volatile materials were removed *in vacuo*. The purple residue was extracted with pentane (50 mL), filtered through a Celite pad (2 × 1 cm), and concentrated to 30 mL. Slow cooling to −80 °C gave analytically pure purple crystals (176 mg, 65.3%) that contained only the trans isomer of **2** (as judged by ^{1}H NMR spectroscopy). ^{1}H NMR: δ 7.04 (br m, 2, aryl), 6.68 (tt, J = 7 Hz, 1 Hz, 1, *para*), 1.06 (s, 15, Cp*), −2.03 (s, 1, NH). $^{13}C\{^1H\}$ NMR (THF-d_8): δ 160.1 (aryl), 128.1 (aryl), 124.3 (aryl), 118.6 (aryl), 98.3 (C_5Me_5), 8.8 (C_5*Me*$_5$). Mp: 197−200 °C dec. IR (Nujol): 3279 (m), 3080 (m), 2728 (w), 2057 (w), 1921 (w), 1833 (w), 1601 (s), 1237 (s), 1209 (m), 1157 (s), 1070 (s), 1025 (s), 996 (m), 944 (w), 883 (m), 816 (s), 758 (m), 690 (s). Anal. Calcd for $C_{32}H_{42}Ni_2N_2$: C, 67.18; H, 7.40; N, 4.90. Found: C, 67.04; H, 7.42; N, 4.89.

[Cp*Ni(μ-NH(2,6-xyl))]$_2$ (3). A flask was charged with Cp*Ni(acac) (370 mg, 1.26 mmol), LiNH(2,6-xyl) (177 mg, 1.39 mmol), and a stir bar and capped with a vacuum adapter. The flask was cooled to −196 °C, THF (30 mL) was condensed into the flask, and the mixture was warmed to −40 °C with stirring. After 30 min, the green solution was allowed to warm to room temperature, and volatile materials were removed *in vacuo*, leaving a purple-brown residue. In the glovebox, the residue was washed with hexamethyldisiloxane (10 mL). The remaining solid was extracted into toluene (75 mL); the resulting solution was filtered through a Celite pad (2 × 1 cm) and the volatile materials were removed to give a purple solid (284 mg, 71.6%), that was judged to be pure **3** (as a mixture of isomers) by ^{1}H NMR

(33) (a) Kolel-Veetil, M. K.; Ahmed, K. J. *Inorg. Chem.* **1994**, *33*, 4945. (b) Kolel-Veetil, M. K.; Curley, J. F.; Yadav, P. R.; Ahmed, K. J. *Polyhedron* **1994**, *13*, 919. (c) Kolel-Veetil, M. K.; Rheingold, A. L.; Ahmed, K. J. *Organometallics* **1993**, *12*, 3439. (d) Casalnuovo, A. L.; Calabrese, J. C.; Milstein, D. *Inorg. Chem.* **1987**, *26*, 971.

(34) (a) Andersen, R. A.; Blom, R.; Boncella, J. M.; Burns, C. J.; Volden, H. C. *Acta Chem. Scand.* **1987**, *A41*, 24. (b) Robbins, J. L.; Edelstein, N.; Spencer, B.; Smart, J. C. *J. Am. Chem. Soc.* **1982**, *104*, 1882.

(35) Charles, R. G.; Pawlikowski, M. A. *J. Phys. Chem.* **1958**, *62*, 440.

(36) Perrin, D. D.; Armarego, W. L. F.; Perrin, D. R. *Purification of Laboratory Materials*; Pergamon: Oxford, 1980.

(37) This product is not very soluble in any common NMR solvent, and only the resonances for the most abundant isomer were observed in the $^{13}C\{^1H\}$ NMR spectrum.

spectroscopy. Analytically pure material could be obtained by crystallization from a mixture of toluene, pentane, and hexamethyldisiloxane. ^{1}H NMR: δ 7.27 (m, 1, aryl), 6.92 (m, 1, aryl), 6.71 (m, 2, aryl), 6.59 (m, 2, aryl), 5.39 (s, 3, C_6H_3(Me)(*Me*), trans), 4.05 (s, 3, C_6H_3(Me)(*Me*), cis), 2.59 (br s, 1, NH, cis), 2.32 (s, 3, C_6H_3(*Me*)(Me), cis), 1.75 (s, 3, C_6H_3(*Me*)(Me), trans), 1.20 (s, 15, C_5Me_5, cis), 0.99 (s, 15, C_5Me_5, trans), −0.11 (br s, 1, NH, trans). ^{13}C{^{1}H} NMR (trans isomer,[37] THF-d_8): δ 131.0 (aryl), 129.3 (aryl), 129.1 (aryl), 127.6 (aryl), 118.5 (aryl), 99.2 (C_5Me_5), 22.9 (C_6H_3(*Me*)(Me)), 19.2 (C_6H_3(Me)(*Me*)), 8.5 (C_5*Me*$_5$). Mp: 247−250 °C dec. IR (C_6D_6): 1589 (m), 1466 (m), 1417 (m), 1250 (m), 1221 (s), 1098 (s), 1020 (m), 758 (s). EI-MS: 313 (100), 506 (46), 626 (30, M^+). Anal. Calcd for $C_{36}H_{50}Ni_2N_2$: C, 68.83; H, 8.02; N, 4.46. Found: C, 68.44; H, 8.30; N, 4.36.

[Cp*Ni(μ-NH^{t}Bu)]$_2$ (4). A Schlenk tube was charged with Cp*Ni(acac) (195 mg, 0.665 mmol), LiNH^{t}Bu (109 mg, 1.38 mmol, 2.07 equiv), and a stir bar. The Schlenk tube was brought out of the box and chilled to −78 °C and THF (10 mL, cooled to −78 °C) was added *via* cannula, with stirring. The orange-brown mixture was warmed to 0 °C and stirred for 20 min, during which time it became brown and homogeneous. The volatile materials were removed at room temperature *in vacuo*. The tube was returned to the glovebox and pentane (25 mL) was added to the green-brown residue. This mixture was filtered through a Celite pad (2 × 1 cm) and the volatile materials were removed from the filtrate *in vacuo*. This crude product was extracted into 120 mL of acetonitrile filtered and the dark green filtrate was cooled slowly to −40 °C. Removal of the supernatant solution and drying *in vacuo* yielded 118 mg (66.7%) of black crystals of **4**. ^{1}H NMR: δ 1.70 (s, 15, C_5Me_5), 1.44 (s, 9, NH^t*Bu*), −5.72 (s, 1, N*H*^{t}Bu). ^{13}C{^{1}H} NMR: δ 97.1 (C_5Me_5), 50.1 (CMe_3), 37.2 (C*Me*$_3$), 10.1 (C_5*Me*$_5$). Mp: 98−100 °C. IR (Nujol): 3263 (w), 2723 (w), 1454 (m), 1352 (m), 1261 (w), 1184 (m), 1157 (w), 1097 (w), 1020 (m), 922 (w), 904 (w), 800 (w), 756 (w), 606 (w), 598 (w), 542 (w). EI-MS: 58 (100), 119 (59), 134 (66), 192 (54), 266 (29), 268 (71), 281 (26), 457 (27), 530 (4, M^+). FAB MS (sulfolane): 250 (47), 265 (69), 457 (100), 530 (67, M^+). Anal. Calcd for $C_{28}H_{50}Ni_2N_2$: C, 63.20; H, 9.47; N, 5.26. Found: C, 63.33; H, 9.32; N, 5.33.

[Cp*Ni(μ-NH^{t}Amyl)]$_2$. The procedure used to prepare **4** was followed, using 141 mg (0.480 mmol) of Cp*Ni(acac), 100 mg (1.07 mmol) of LiNH^{t}Amyl, and 8 mL of THF. The solution was stirred for 10 min, extracted with 20 mL of pentane, and crystallized from 80 mL of acetonitrile, giving 63.6 mg (47.5%) of black plates of [Cp*Ni(μ-NH^{t}Amyl)]$_2$. Although this material appeared to be pure by ^{1}H NMR, several attempts to obtain satisfactory elemental analyses were unsuccessful. ^{1}H NMR: δ 1.74 (s, 15, C_5Me_5), 1.47 (s, C*Me*$_2$CH$_2$CH$_3$), 1.47 (q, J = 7.5 Hz, CMe$_2$C*H*$_2$CH$_3$), 0.84 (t, 9, J = 7.5 Hz, CMe$_2$CH$_2$C*H*$_3$), −5.67 (s, 1, N*H*^{t}Bu). ^{13}C{^{1}H} NMR: δ 98.2 (C_5Me_5), 53.2 (*C*Me$_2$CH$_2$CH$_3$), 42.2 (CMe$_2$*C*H$_2$CH$_3$), 33.2 (C*Me*$_2$CH$_2$CH$_3$), 11.2 (CMe$_2$CH$_2$*C*H$_3$), 10.3 (C_5*Me*$_5$). Mp: >250 °C. IR (Nujol): 3257 (w), 2719 (m), 1574 (w), 1516 (w), 1352 (m), 1315 (w), 1286 (m), 1261 (m), 1173 (m), 1147 (s), 1059 (m), 1020 (s), 935 (m), 874 (m), 800 (m), 727 (m). Anal. Calcd for $C_{30}H_{54}Ni_2N_2$: C, 64.32; H, 9.72; N, 5.00. Found: C, 63.79; H, 9.80; N, 4.88.

Preparation of a Mixture of [Cp*Ni(μ-NH^{t}Bu)]$_2$ (4), [Cp*Ni(μ-NH^{t}Amyl)]$_2$, and Cp*Ni(μ-NH^{t}Bu)(μ-NH^{t}Amyl)NiCp*. The procedure used to prepare **5** was followed, using 166 mg (0.567 mmol) of Cp*Ni(acac), 50 mg (0.63 mmol, 1.1 equiv) of LiNH^{t}Bu, and 62 mg (0.67 mmol, 1.2 equiv) of LiNH^{t}Amyl for the reaction and a mixture of 60 mL of acetonitrile and 25 mL of propionitrile for the crystallization. This gave a mixture (1:1:2) of the amides as black crystals. ^{1}H NMR (all integrations referenced to **4**): δ 1.74 (s, 15, C_5Me_5 of [Cp*Ni(μ-NH^{t}Amyl)]$_2$), 1.72 (s, 30, C_5Me_5 of mixed product), 1.70 (s, 15, C_5Me_5 of **4**), 1.47 (s, 9, methyl), 1.45 (m, 2 × CMe$_2$C*H*$_2$CH$_3$), 1.44 (s, 9, methyl), 1.43 (s, 9, methyl), 0.84 (dt, 6, J = 7.5 Hz, 2 × CMe$_2$CH$_2$C*H*$_3$), −5.61 (s, 1, N*H* of mixed product), −5.67 (s, 1, N*H* of [Cp*Ni(μ-NH^{t}Amyl)]$_2$), −5.71 (s, 1, N*H* of **4**), −5.77 (s, 1, N*H* of mixed product).

Preparation of a Mixture of 1, 3, and Cp*Ni(μ-NH(*p*-tol))(μ-NH(2,6-xylyl))NiCp*. The procedure used to prepare **1** was followed, using 107 mg (0.365 mmol) of Cp*Ni(acac), 22.7 mg (0.201 mmol, 0.55 equiv) of LiNH(*p*-tol), 25.4 mg (0.200 mmol, 0.55 equiv) of LiNH(2,6-xylyl), and 20 mL of THF for the reaction and 25 mL pentane for the crystallization. This gave a mixture of the mixed amide and **3** as a dark solid. ^{1}H NMR (all integrations referenced to *trans*-**3**): δ 7.41 (m, 0.4, aryl), 7.27 (m, 1.5, aryl), 6.91 (m, 1, aryl), 6.71 (m, 2, aryl), 6.60 (m, 2, aryl), 5.39 (s, 3, *trans*-**3**), 5.17 (s, 0.6, mixed product), 4.95 (s, 0.6, mixed product), 4.05 (s, 2.3, *cis*-**3**), 2.59 (s, 0.4, *cis*-**3**), 2.32 (s, 2.3, *cis*-**3**), 2.16 (s, 0.7, mixed product), 2.11 (s, 0.7, mixed product), 2.06 (s, 0.6, mixed product), 1.87 (s, 0.7, mixed product), 1.75 (s, 3, *trans*-**3**), 1.41 (s, 0.2, mixed product), 1.20 (s, 11, *cis*-**3**), 1.06 (s, 6, mixed product), 1.03 (s, 6, mixed product), 0.99 (s, 15, *trans*-**3**), 0.36 (s, 0.2, mixed product), −0.11 (s, 1, *trans*-**3**), −0.70 (s, 0.2, mixed product), −2.41 (s, 0.2, mixed product). Heating a solution of this mixture in THF-d_8 to 105 °C for several hours did not result in any isomerization, although ^{1}H NMR indicated that significant decomposition had taken place.

Cp^{Et}Ni(acac). A solution of Cp$^{Et}{}_2$Mg (520 mg, 1.61 mmol) in THF (15 mL) was added to a slurry of Ni(acac)$_2$ in THF (10 mL) (Cp^{Et} = C_5Me_4Et). This caused an immediate color change from green to deep red. This solution was stirred for 90 min, and volatile materials were removed *in vacuo*. The resulting dark red residue was extracted with diethyl ether (25 mL), filtered through a Celite pad (2 × 1 cm), and concentrated to 7 mL. Slow cooling to −80 °C gave dark red crystals (576 mg, 58.3%) that were suitable for synthesis. Sublimation at 70 °C onto a 5 °C cold finger gave analytically pure material. ^{1}H NMR (C_6D_6, 298 K): δ 64.4 (br s, $\nu_{1/2}$ = 76 Hz, 6, Cp^{Et} methyls), 60.9 (br s, $\nu_{1/2}$ = 69 Hz, 6, Cp^{Et} methyls), 33.3 (br s, $\nu_{1/2}$ = 31 Hz, 2, Cp^{Et} ethyl), 5.0 (br s, $\nu_{1/2}$ = 15 Hz, 3, Cp^{Et} ethyl), −2.3 (s, $\nu_{1/2}$ = 6 Hz, 6, acac methyls), −10.1 (s, $\nu_{1/2}$ = 11 Hz, 1, acac methine). Mp: 74.5−75.5 °C. IR (Nujol): 3077 (sh), 2741 (w), 1599 (s), 1518 (s), 1261 (m), 1198 (m), 1155 (m), 1080 (w), 1055 (w), 1020 (m), 928 (m), 796 (m), 766 (w), 660 (m), 623 (m). μ_{eff} (298 K): 1.2 μ_B. Anal. Calcd for $C_{16}H_{24}NiO_2$: C, 62.58; H, 7.88. Found: C, 62.37; H, 8.05.

[Cp^{Et}Ni(μ-NH(*p*-tol))]$_2$ (1′). A flask was charged with Cp^{Et}Ni(acac) (275 mg, 0.895 mmol), LiNH(*p*-tol) (105 mg, 0.928 mmol), and a stir bar and capped with a vacuum adapter. The flask was cooled to −196 °C, THF (30 mL) was condensed into the flask, and the mixture was warmed to −78 °C with stirring. The blue solution was allowed to warm to room temperature over 1 h with stirring. The volatile materials were removed *in vacuo*, leaving a brown residue. In the glovebox, the residue was extracted into pentane (65 mL); the resulting solution was filtered through a Celite pad (2 × 1 cm) and concentrated to 15 mL. Slow cooling to −80 °C gave purple crystals (153 mg, 54.4%) of **1′** that contained a roughly 1:1 mixture of isomers (as judged by ^{1}H NMR spectroscopy). Analytically pure material was obtained by recrystallization from pentane. ^{1}H NMR: δ 7.61 (m, aryls), 6.88 (m, aryls), 2.15 (s, 3, C_6H_4Me, trans), 2.12 (s, 3, C_6H_4Me, cis), 1.97 (q, J = 7.6 Hz, 2, Cp^{Et} ethyl, cis), 1.88 (m, 2, Cp^{Et} ethyl, trans), 1.36 (s, 3, Cp^{Et} methyl, trans), 1.17 (s, *ca.* 6, Cp^{Et} methyls, cis), 1.17 (t, J = 7.5 Hz, *ca.* 3, Cp^{Et} ethyl), 1.04 (t, J = 7.5 Hz, 3, Cp^{Et} ethyl), 1.02 (s, 3, Cp^{Et} methyl, trans), 0.99 (s, 3, Cp^{Et} methyl, trans), 0.90 (s, 6, Cp^{Et} methyls, cis), 0.84 (s, 3, Cp^{Et} methyl, trans), −1.91 (s, 1, NH, cis), −2.01 (s, 1, NH, trans). ^{13}C{^{1}H} NMR: δ 156.1 (aryl), 155.4 (aryl), 128.6 (aryl), 127.2 (aryl), 127.1 (aryl), 123.5 (aryl), 123.3 (aryl), 106.1 (C_5Me_4Et), 105.4 (C_5Me_4Et), 100.8 (C_5Me_4Et), 98.6 (C_5Me_4Et), 97.2 (C_5Me_4Et), 96.4 (C_5Me_4Et), 94.1 (C_5Me_4Et), 20.7 (C_6H_4Me), 20.7 (C_6H_4Me), 17.6 ($C_5Me_4CH_2CH_3$), 17.6 ($C_5Me_4CH_2CH_3$), 15.5 (Cp^{Et} methyl), 15.0 (Cp^{Et} methyl), 9.0 (Cp^{Et} methyl), 8.8 (Cp^{Et} methyl), 8.8 (Cp^{Et} methyl), 8.6 (Cp^{Et} methyl), 8.6 (Cp^{Et} methyl), 8.6 (Cp^{Et} methyl). Mp: 151−153 °C. IR (Nujol): 3278 (w), 2734 (w), 1869 (m), 1749 (w), 1611 (s), 1270 (s), 1102 (m), 1022 (s), 966 (w), 939 (w), 817 (m), 748 (w), 710 (w). Anal. Calcd for $C_{36}H_{50}Ni_2N_2$: C, 68.83; H, 8.02; N, 4.46. Found: C, 69.05; H, 8.08; N, 4.39.

[Cp^{Et}Ni(μ-NH(2,6-xylyl))]$_2$ (3′). A flask was charged with Cp^{Et}Ni(acac) (191 mg, 0.623 mmol), LiNH(2,6-xylyl) (90 mg, 0.71 mmol), and a stir bar and capped with a vacuum adapter. The flask was cooled to −196 °C, THF (30 mL) was condensed into the flask, and the mixture was warmed to −40 °C with stirring. After 30 min, the blue-green solution was allowed to warm to 0 °C, and volatile materials were removed *in vacuo*, leaving a purple-brown residue. In the glovebox, the residue was extracted into pentane (60 mL); the resulting solution was filtered through a Celite pad (2 × 1 cm) and concentrated to 15 mL. Slow cooling to −80 °C gave purple crystals (113 mg, 55.4%) of **3′** as a roughly 1:1 mixture of isomers (as judged by ^{1}H NMR spectroscopy). Although recrystallization gave material that appeared

pure by NMR spectroscopy, repeated attempts at elemental analysis gave unsatisfactory results (see below). ^{1}H NMR: δ 7.28 (d, $J = 7$ Hz, 1, aryl), 6.9 (m, 2, aryl), 6.72 (t, $J = 7$ Hz, 1, aryl), 6.62 (d, $J = 7$ Hz, 1, aryl), 5.41 (s, 3, C_6H_3*(Me)*(Me), trans), 4.09 (s, 3, C_6H_3*(Me)*(Me), cis), 2.64 (s, 1, NH, cis), 2.34 (s, 3, C_6H_3(Me)*(Me)*, cis), 1.80 (m, $C_5Me_4CH_2CH_3$, cis), 1.77 (s, 3, C_6H_3(Me)*(Me)*, trans), 1.67 (q, $J = 7$ Hz, 2, $C_5Me_4CH_2CH_3$, trans), 1.27 (s, 6, C_5Me_4Et, cis), 1.14 (s, 6, C_5Me_4-Et, cis), 1.06 (s, 3, C_5Me_4Et, trans), 0.99 (s, 3, C_5Me_4Et, trans), 0.97 (s, 3, C_5Me_4Et, trans), 0.93 (s, 3, C_5Me_4Et, trans), 0.79 (t, $J = 7$ Hz, 3, $C_5Me_4CH_2CH_3$, cis), 0.74 (t, $J = 8$ Hz, 3, $C_5Me_4CH_2CH_3$, trans), −0.06 (s, 1, NH, trans). ^{13}C{^{1}H} NMR (THF-d_8): δ 152.4 (aryl), 150.4 (aryl), 130.9 (aryl), 129.9 (aryl), 129.2 (aryl), 129.0 (aryl), 128.4 (aryl), 127.7 (aryl), 127.5 (aryl), 118.9 (aryl), 118.5 (aryl), 105.1 (C_5Me_4Et), 101.8 (C_5Me_4Et), 100.7 (C_5Me_4Et), 99.7 (C_5Me_4Et), 98.7 (C_5Me_4Et), 97.7 (C_5Me_4Et), 97.2 (C_5Me_4Et), 22.9 (C_6H_3*(Me)*(Me), trans), 22.5 (C_6H_3*(Me)*-(Me), cis), 19.5 (C_6H_3(Me)*(Me)*, cis), 19.2 (C_6H_3(Me)*(Me)*, trans), 17.6 ($C_5Me_4CH_2CH_3$, trans), 17.1 ($C_5Me_4CH_2CH_3$, cis), 14.2 (Cp^{Et} methyl), 8.5 (Cp^{Et} methyl), 8.3 (Cp^{Et} methyl), 8.2 (Cp^{Et} methyl), 8.0 (Cp^{Et} methyl), 7.7 (Cp^{Et} methyl). Mp: 219−220 °C dec. IR (Nujol): 3305 (w), 3284 (w), 2734 (w), 1896 (w), 1588 (s), 1411 (m), 1330 (m), 1251 (s), 1218 (s), 1155 (m), 1096 (s), 1020 (s), 984 (m), 837 (m), 755 (m). Anal. Calcd for $C_{30}H_{54}Ni_2N_2$: C, 69.55; H, 8.29; N, 4.27. Found: C, 69.17; H, 8.41; N, 4.72. EI-MS: 106 (46), 121 (100), 327 (30), 534 (64), 654 (45, M^+). High-resolution EI-MS: Calcd ($^{58}Ni_2$/$^{58}Ni^{60}Ni$): 654.2994/656.2948. Found: 654.2986/656.2956.

[Cp^{Et}Ni(μ-NH^{t}Bu)]$_2$ (4′). A flask was charged with Cp^{Et}Ni(acac) (193 mg, 0.628 mmol), LiNH^{t}Bu (56 mg, 0.71 mmol), and a stir bar and capped with a vacuum adapter. The flask was cooled to −196 °C, THF (30 mL) was condensed into the flask, and the mixture was warmed to −78 °C with stirring. After 30 min, the blue-green solution was allowed to warm to −40 °C, and the volatile materials were removed *in vacuo*, leaving a purple-red residue. In the glovebox, the residue was extracted into pentane (40 mL); the resulting solution was filtered through a Celite pad (2 × 1 cm) and concentrated to 4 mL. Slow cooling to −30 °C gave large black crystals of **4′** in a yield of 65.5 mg (37.2%). Attempts to collect further crops gave only brown solids. ^{1}H NMR: δ 2.22 (q, $J = 7.4$ Hz, 2, $C_5Me_4CH_2CH_3$), 1.74 (s, 6, $C_5Me_4CH_2CH_3$), 1.72 (s, 6, $C_5Me_4CH_2CH_3$), 1.45 (s, 9, CMe_3), 1.04 (t, $J = 7.4$ Hz, 3, $C_5Me_4CH_2CH_3$), −5.71 (s, 1, N*H*). ^{13}C{^{1}H} NMR: δ 103.4 (C_5Me_4Et), 98.9 (C_5Me_4Et), 97.2 (C_5Me_4Et), 51.0 (CMe_3), 37.5 (CMe_3), 19.1 ($C_5Me_4CH_2CH_3$), 15.2 (Cp^{Et} methyl), 10.4 (Cp^{Et} methyl), 10.2 (Cp^{Et} methyl). Mp: 102−103.5 °C dec. IR (Nujol): 3260 (w), 2719 (w), 1455 (sh), 1354 (sh), 1304 (m), 1261 (w), 1181 (s), 1155 (s), 1047 (m), 1018 (s), 968 (m), 955 (m), 919 (m), 906 (s), 788 (m), 754 (m). Anal. Calcd for $C_{30}H_{54}Ni_2N_2$: C, 64.32; H, 9.72; N, 5.00. Found: C, 64.34; H, 9.86; N, 4.97.

Reaction of 4 with CO. In a glovebox, **4** (4.3 mg, 8.1 μmol) was placed in a vial and C_6D_6 (0.6 mL) was added. The green-black solution was transferred to a J. Young NMR tube, which was closed, brought out of the glovebox, and degassed with two freeze/pump/thaw cycles. The tube was repressurized to 1 atm with CO and the tube was shaken and monitored by ^{1}H NMR spectroscopy. Over several days at room temperature, the solution changed to a red color and new peaks increased in intensity. After 3 weeks at room temperature, the ^{1}H NMR spectrum showed a large resonance at δ 1.75 ppm due to [Cp*Ni(μ-CO)]$_2$ (lit. δ 1.75 ppm),[28] and other resonances at δ 5.33 (s, 2), 3.18 (br s, 1), 1.68 (t, 12), 1.28 (s, 9), 1.09 (br s, *ca.* 15), and 0.59 (s, 1) ppm (integrations referenced to [Cp*Ni(μ-CO)]$_2$ = 15). After removal of volatile materials and dissolution in C_6D_6, ^{1}H NMR resonances remained for [Cp*Ni(μ-CO)]$_2$ and another nonvolatile product (resonances at δ 3.18, 1.28), in addition to some unreacted starting material. Dissolution in diethyl ether and filtration through a silica plug removed starting material, but left the other nonvolatile products unchanged, as determined by ^{1}H NMR spectroscopy. IR (C_6H_{12} solution): 1857 (s), 1815 (vs). (Lit. for [Cp*Ni(μ-CO)]$_2$ in C_6H_{12}: 1857, 1815.)[28]

Cp*Ni(CO)(C(O)NH(*p*-tol)) (6). In a glovebox, **1** (26 mg, 43 μmol) was dissolved in toluene (75 mL) and placed in a flask with a stir bar. This purple solution was brought out of the box, frozen, and degassed and CO (250 Torr) was expanded into the headspace (*ca.* 30 mL). The solution was warmed to 0 °C and stirred for 10 h, over which time it turned clear red. The volatile materials were then removed *in vacuo*. The residue was washed with hexamethyldisiloxane (10 mL) to give a red solution that was found to contain almost exclusively [Cp*Ni(μ-CO)]$_2$, as judged by ^{1}H NMR spectroscopy. The light orange residue was dissolved in diethyl ether (10 mL), filtered, and dried *in vacuo* to give analytically pure **6** as a light orange powder (12 mg, 39%). ^{1}H NMR: δ 7.35 (d, $J = 8$ Hz, 2, aryl), 6.90 (d, $J = 8$ Hz, 2, aryl), 6.67 (br s, 1, NH), 2.05 (s, 3, C_6H_4Me), 1.65 (s, 15, C_5Me_5). IR (C_6D_6): 3147 (w), 2015 (vs), 1647 (s), 1511 (m), 1472 (m), 1390 (w), 1286 (m), 1224 (m), 1081 (s), 865 (w). Anal. Calcd for $C_{19}H_{23}NiNO_2$: C, 64.08; H, 6.51; N, 3.93. Found: C, 64.01; H, 6.68; N, 4.08. When this powder was left at room temperature for several days, it turned red, and ^{1}H NMR spectroscopy confirmed production of [Cp*Ni(μ-CO)]$_2$.[28]

Cp*Ni(^{13}CO)(^{13}C(O)NH(*p*-tol)). This was synthesized in a fashion analogous to that used for the natural-abundance sample above, except that the reaction was performed in an NMR tube with 5 mg of **1**, 0.6 mL of C_6D_6, and 375 Torr of ^{13}CO, in order to monitor the reaction at room temperature. Similar workup yielded Cp*Ni(^{13}CO)(^{13}CONH(*p*-tol)) as an orange solid. ^{13}C{^{1}H} NMR: δ 192.4 (d, $^2J_{CC} = 9$ Hz, Ni-*C*O), 185.2 (br s, $\nu_{1/2} = 22$ Hz, *C*(O)NH(*p*-tol)).

Decomposition of 6 in Solution. In the glovebox, **6** (4 mg) was placed in a vial and C_6D_6 (0.6 mL) was added. The orange solution was transferred to an NMR tube, which was placed on a Cajon adapter, brought out of the glovebox, frozen at −196 °C, degassed, and flame sealed. The tube was warmed to room temperature and monitored by ^{1}H NMR spectroscopy. After 2 days at room temperature, the red solution was almost exclusively [Cp*Ni(μ-CO)]$_2$ (*vide supra*), and a white powder had appeared. Repetition of the reaction on a larger scale (*ca.* 20 mg of **6**) gave enough white powder to allow ^{1}H NMR and IR analysis. ^{1}H NMR ($CDCl_3$): δ 7.22 (d, $J = 8.4$ Hz, 2, aryl), 7.14 (d, $J = 8.3$ Hz, 2, aryl), 6.44 (br s, 1, N*H*(*p*-tol)), 2.33 (s, 3, C_6H_4Me). IR (KBr): 3306 (m), 1637 (vs), 1593 (s), 1563 (s). For a sample of ((*p*-tol)NH)$_2$C=O prepared independently by mixing pentane/toluene (6:1) solutions of *p*-toluidine (684 mg, 6.38 mmol) and *p*-tolyl isocyanate (854 mg, 6.41 mmol), filtering through a glass frit, and washing the white solid with pentane, all ^{1}H NMR and IR resonances were identical except the N*H* resonance in the ^{1}H NMR spectrum, which resonated at δ 6.50 ppm in the authentic sample.

Reaction of 4 with ^{t}BuNC. In the glovebox, **4** (5.8 mg, 11 μmol) was placed in a vial and C_6D_6 (0.6 mL) was added. *tert*-Butyl isonitrile (12.5 μL, 110 μmol) was added to the solution *via* syringe. The greenish-black solution was transferred to an NMR tube, which was placed on a Cajon adapter, brought out of the glovebox, frozen at −196 °C, degassed, flame sealed, warmed to room temperature, and monitored by ^{1}H NMR spectroscopy. After 2 days at room temperature, the product was almost exclusively Ni(CN^{t}Bu)$_4$ (*vide infra*); no other products or intermediates were detected.

Reaction of 3 with tBuNC. In the glovebox, **3** (3.4 mg, 5.4 μmol) was placed in a vial and C_6D_6 (0.6 mL) was added. The purple solution was transferred to an NMR tube, which was placed on a Cajon adapter, brought out of the glovebox, frozen at −196 °C, and degassed. *tert*-Butyl isonitrile (23.58 mL at 21.3 Torr, 16.8 μmol) was condensed into the tube, which was then flame sealed, warmed to room temperature, and monitored by ^{1}H NMR spectroscopy. After 1 day at room temperature, the product was almost exclusively Ni(CN^{t}Bu)$_4$ (*vide infra*), and no other products or intermediates were detected.

Cp*Ni(CN^{t}Bu)(C(N^{t}Bu)NH(*p*-tol)) (7). In the glovebox, a solution of **1** (32.6 mg, 54.3 μmol) and ^{t}BuNC (18.0 mg, 217 μmol) in toluene (7 mL) was stirred for 4 h, and then the volatile materials were removed *in vacuo*. The brown residue was dissolved in pentane (4 mL), filtered, concentrated to 1 mL, and cooled slowly to −30 °C. The cold solution gave a small quantity of orange crystals of Ni(CN^{t}Bu)$_4$ (^{1}H NMR (C_6D_6): δ 1.09 (s). Lit. (toluene-d_8, −20 °C):[38a] δ 1.03 (s). IR (C_6D_6): 2023 cm^{-1}. Lit. (C_6H_6):[38b] 2026 cm^{-1}) and a brown solution. The brown supernatant was evaporated *in vacuo* to give a brown residue (32 mg, 63%) of **7** in >90% purity. Silica chromatography using

(38) (a) Otsuka, S.; Nakamura, A.; Tatsuno, Y. *J. Am. Chem. Soc.* **1969**, *91*, 6994. (b) Nast, R.; Schulz, H.; Moerler, H.-D. *Chem. Ber.* **1970**, *103*, 777.

(39) Tolman, C. A. *J. Am. Chem. Soc.* **1970**, *92*, 2956.

(40) Amman, C.; Meier, P.; Merbach, A. E. *J. Magn. Reson.* **1982**, *46*, 319.

(41) Kaleidagraph v.2.1.3, Abelbeck Software, 1991.

pentane/diethyl ether as eluent gave analytically pure **7**. ^{1}H NMR: δ 7.41(d, J = 8 Hz, 2, aryl), 7.20 (d, J = 8 Hz, 2, aryl), 4.42 (br s, 1, NH), 2.34 (s, 3, C_6H_4*Me*), 1.71 (s, 15, C_5Me_5), 1.57 (s, 9, C(N^t*Bu*)-NH(*p*-tol)), 0.92 (s, 9, Ni-CN^t*Bu*). ^{13}C{^{1}H} NMR: δ 172.5 (Ni-*C*N^t-Bu), 151.9 (Ni-*C*N^{t}Bu), 139.5 (aryl), 128.7 (aryl), 128.5 (aryl), 122.7 (aryl), 100.0 (*C*$_5$Me$_5$), 52.6 (*C*Me$_3$), 30.5 (C*Me*$_3$), 29.7 (C*Me*$_3$), 21.1 (C_6H_4*Me*), 10.2 (C_5*Me*$_5$). Mp: 100−103 °C. IR (C_6D_6): 3441 (vw), 3233 (vw), 2120 (vs), 1557 (vs), 1502 (s), 1465 (m), 1432 (s), 1382 (m), 1356 (m), 1232 (m), 1212 (m), 1132 (s), 882 (m). EI-MS: 309 (39), 382 (100), 465 (45, M$^+$). Anal. Calcd for $C_{27}H_{41}NiN_3$: C, 69.54; H, 8.86; N, 9.01. Found: C, 69.37; H, 9.10; N, 8.84.

Cp*Ni(PMe$_3$)(NH(*p*-tol)) (5). In the glovebox, **1** (5.2 mg, 8.7 μmol) was placed in a vial and C_6D_6 (0.6 mL) was added. The purple solution was transferred to an NMR tube, which was placed on a Cajon adapter, brought out of the glovebox, frozen at −196 °C, and degassed. Trimethylphosphine (6.6 mL at 54 Torr, 19 μmol) was condensed into the tube, which was then flame sealed, warmed to room temperature, and monitored by ^{1}H and ^{31}P{^{1}H} NMR spectroscopy. After 10 h at room temperature, the product was almost exclusively Cp*Ni(PMe$_3$)-(NH(*p*-tol)) (**5**). Attempts to isolate this complex from solution invariably resulted in partial conversion to a mixture of **1** and Ni(PMe$_3$)$_4$ (^{1}H NMR (C_6D_6): δ 1.15 (s). ^{31}P NMR (C_6D_6): δ −21.4. Lit. (toluene-d_8):[39] δ 1.17 (s), δ −22.2). For **5**, ^{1}H NMR: δ 6.99 (d, J = 8 Hz, 2, aryl), 6.87 (d, J = 8 Hz, 2, aryl), 2.35 (s, 3, C_6H_4*Me*), 1.52 (d, J_{PH} = 1.6 Hz, 15, C_5Me_5), 0.73 (d, J_{PH} = 9 Hz, 9, PMe$_3$), −1.05 (br s, 1, NH). ^{13}C{^{1}H} NMR: δ 158.6 (aryl), 129.6 (aryl), 123.7 (aryl), 117.7 (aryl), 100.5 (*C*$_5$Me$_5$), 15.1 (C_6H_4*Me*), 10.2 (C_5*Me*$_5$). ^{31}P{^{1}H} NMR: δ -5.9.

Reaction of 1 with Aniline. In the glovebox, **1** (5.3 mg, 8.8 μmol) was placed in a vial and C_6D_6 (0.6 mL) was added. Aniline (1 drop, excess) was added to the solution *via* pipet. The purple solution was transferred to an NMR tube, which was placed on a Cajon adapter, brought out of the glovebox, frozen at −196 °C, degassed, flame sealed, warmed to room temperature, and monitored by ^{1}H NMR spectroscopy. After 15 h at room temperature, the solution contained mostly **2** and *ca.* 0.5 equiv of Cp*Ni(μ-NH(*p*-tol))(μ-NHPh)NiCp*. ^{1}H NMR (mixed product, as cis and trans isomers): δ 2.06 (s, C_6H_4*Me*), 2.01 (s, C_6H_4*Me*), 1.08 (s, Cp*), 1.07 (s, Cp*), −1.73 (s, NH), −2.02 (s, NH). Detection of aryl resonances and accurate integrations were impossible due to significant overlap of the mixed product peaks with those from other reactants and products.

Crossover of 1 and 2. In the glovebox, **2** (8.4 mg, 14.7 μmol) and **1** (8.5 mg, 14.2 μmol) were placed in a vial and C_6D_6 (0.5 mL) was added. The purple solution was transferred to an NMR tube, which was placed on a Cajon adapter, brought out of the glovebox, frozen at −196 °C, flame sealed, warmed to room temperature, and monitored by ^{1}H NMR spectroscopy. After 1 week at 45 °C, the solution was a mixture (*ca.* 1:1:1) of **1**, **2**, and Cp*Ni(μ-NH(*p*-tol))(μ-NHPh)NiCp* (*vide supra*). Further heating resulted in a *ca.* 1:1:2 ratio of compounds. After several weeks at 45 °C, the solvent was evaporated to give a purple powder that was used for EI-MS characterization. EI-MS: 93 (75), 106 (100), 192 (24), 285 (18), 299 (33), 477 (34), 491 (36), 570 (14, M$^+$, **2**), 584 (26, M$^+$, mixed product), 598 (15, M$^+$, **1**).

Rates of Isomerization. All kinetic runs were performed using variants of the following procedure. In the glovebox, *trans*-**2** (5.0 mg), ferrocene (1.7 mg), and Cp_2ZrMe_2 (0.7 mg) were dissolved in THF-d_8 (0.4 mL) and transferred to a new medium-wall NMR tube. The tube was placed on a Cajon adapter, brought out of the glovebox, frozen at −196 °C (but *not* degassed), and flame sealed. The NMR probe was warmed to 76.9 °C, as determined from a peak separation in an ethylene glycol standard sample of 1.143 ppm.[40] The T_1's of the protons were checked, and they were all invariably shorter than 15 s. The sample was inserted into the probe and scans with a 90° pulse width were recorded every 6 min. Integrations were determined vs the ferrocene resonance at δ 4.0 ppm. Rates and errors were determined by exponential curve-fitting on KaleidaGraph.[41] Plots of log $|[A] - [A]_{eq}|$ vs time were always linear to 3 half-lives, after which time the noise often made line-fitting difficult; in several cases, however, the lines were linear to >5 half-lives.

X-ray Crystal Structure of 1′. A mixture of clear purple blocky and flakelike crystals of **1′** were obtained by slow cooling of a concentrated pentane solution. The data collection methods used here have been described.[42] The final cell parameters and specific data collection parameters for this data set are given in Table 6 and the supporting information. The 2919 raw intensity data were converted to structure factor amplitudes as described earlier.[42] Inspection of the azimuthal scan data[43] showed a variation I_{min}/I_{max} = 0.95 for the average curve. An empirical correction based on the observed variation was applied to the data. The choice of space group *C*2/*c* was confirmed by inspection of the systematic absences and the successful solution and refinement of the structure. The structure was solved by Patterson methods and refined via standard least-squares and Fourier techniques. Hydrogen atoms were assigned idealized locations and values of B_{iso} approximately 1.25 times the B_{equiv} of the atoms to which they were attached. They were included in structure factor calculations, but not refined. The final residuals for the 2051 data for which $F^2 > 3\sigma(F^2)$ were R = 4.20%, wR = 5.15%, and GOF = 1.64. The R value for all 2812 data was 6.49%. The maximum and minimum peaks on the final difference Fourier map corresponded to 0.38 and −0.37 e$^-$/Å^3, respectively. Data reduction and refinement formulae, anisotropic thermal parameters, and the positional parameters of all atoms are available as supporting information.

Table 6. Selected Crystal and Data Parameters for *cis*-**1′**, *trans*-**3′**, and **4′**

	cis-**1′**	*trans*-**3′**	**4′**
formula	$C_{36}H_{50}Ni_2N_2$	$C_{38}H_{54}Ni_2N_2$	$C_{30}H_{54}Ni_2N_2$
a (Å)	17.574(5)	8.4268(5)	19.7934(1)
b (Å)	16.360(3)	10.6600(6)	9.1003(1)
c (Å)	11.102(2)	10.9110(7)	17.9028(2)
α (deg)	90	115.251(1)	90
β (deg)	91.18(2)	102.957(1)	113.616(1)
γ (deg)	90	98.529(1)	90
V (Å^3)	3191.3(20)	830.16(8)	2954.69(5)
space group	$C2/c$ (C_{2h}^6, #15)	$P\bar{1}$ (C_i^1, #2)	$C2/c$ (C_{2h}^6, #15)
Z	4	1	4
diffractometer	CAD4	Siemens SMART	Siemens SMART
detector	crystal scintillation counter, with PHA	CCD area detector	CCD area detector
temp (°C)	−90 ± 1	−140 ± 2	−138 ± 1
no. of unique reflctns	2812	2318	4490[a]
T_{min}/T_{max}	0.95	0.45	0.93
no. of variables	181	271	235
R; R_w	0.042; 0.052	0.054, 0.063	0.029; 0.043
R (including zeros)	0.065	0.065	0.031
goodness of fit indicator	1.64	2.09	1.95

[a] Includes systematic absences.

X-ray Crystal Structure of 3′. An irregularly-shaped purple plate of **3′** (approximate dimensions 0.25 × 0.20 × 0.08 mm) was obtained by cooling a pentane solution to −30 °C. The crystal was mounted on a glass fiber using Paratone N hydrocarbon oil and centered on the beam. It was cooled to −140 °C by a nitrogen flow low-temperature apparatus that had been previously calibrated by a thermocouple placed at the sample position. All measurements were made on a Siemens SMART diffractometer with a CCD area detector[45a] using graphite monochromated Mo Kα radiation.

Good crystal quality was confirmed by well-shaped, intense spots appearing to $2\theta \geq 45°$. Collection of 60 10-s frames, followed by spot integration and least-squares refinement, gave a preliminary orientation matrix and cell constants. A full hemisphere of reciprocal space was measured, using 20-s frames of width 0.3° in ω. The raw data were integrated (XY spot spread = 1.60°; Z spot spread = 0.60°) using SAINT.[45b] The unit cell parameters were refined, giving the final values shown in Table 6 and the supporting information. Data analysis was performed using Siemens XPREP.[45c] The unit cell parameters indicated a primitive triclinic cell; the choice of $P\bar{1}$ was confirmed by

(42) Dobbs, D. A.; Bergman, R. G. *Inorg. Chem.* **1994**, *33*, 5329.

(43) Reflections used for azimuthal scans were located near χ = 90° and the intensities were measured at 10° increments of rotation of the crystal about the diffraction vector.

(44) Cromer, D. T.; Waber, J. T. *International Tables for X-ray Crystallography*; The Kynoch Press: Birmingham, England, 1974; Vol. IV.

successful solution and refinement of the structure. The data were corrected for Lorentz and polarization effects. No correction for decomposition was necessary, but a semiempirical ellipsoidal absorption correction ($T_{max} = 0.842$, $T_{min} = 0.381$) was applied.

Of the 3353 reflections that were measured, 2318 were unique ($R_{int} = 10.5\%$); equivalent reflections were merged. The structure was solved and refined with the teXsan software package[45d] using direct methods[45e] and expanded using Fourier techniques.[45f] The non-hydrogen atoms were refined anisotropically. The hydrogen atoms were located in a Fourier synthesis; their coordinates were refined but their isotropic *B*'s were held fixed at 2.5. The final cycle of full-matrix least-squares refinement was based on 1967 observed reflections ($I > 3\sigma(I)$) and 271 variable parameters and converged with unweighted and weighted agreement factors of $R = 5.4\%$, $R_w = 6.3\%$ and GOF = 2.09. Using all 2318 unique data (including systematic absences), $R = 6.5\%$ and $R_w = 6.6\%$. The weighting scheme was based on counting statistics and included a factor ($p = 0.030$) to downweight the intense reflections. Neutral atom scattering factors and mass attenuation coefficients were given standard values.[44,45g] Anomalous dispersion effects were included in F_{calc}.[45g,h] The maximum and minimum peaks on the final difference Fourier map corresponded to 0.63 and -1.06 $e^-/Å^3$, respectively. Data reduction and refinement formulae, anisotropic thermal parameters, and positional parameters for all atoms are available as supporting information.

X-ray Crystal Structure of 4′. A large black block of **4′** was obtained by cooling a pentane solution to -30 °C. A shard ($0.20 \times 0.21 \times 0.26$ mm) was cleaved from the large crystal and mounted. The data collection, reduction, and refinement were carried out as described for **3′**, using the data collection, reduction, and refinement parameters in Table 6, except for the following changes. Inspection of the systematic absences revealed a monoclinic C-centered cell, with possible space groups *Cc* and *C*2/*c*; the choice of *C*2/*c* was confirmed by successful solution and refinement of the structure. Least-squares refinement converged with unweighted and weighted agreement factors of $R = 2.9\%$, $R_w = 4.3\%$, and GOF = 1.95. Using all unique data (including systematic absences), $R = 3.1\%$, $R_w = 4.4\%$. The maximum and minimum peaks on the final difference Fourier map corresponded to 0.28 and -0.32 $e^-/Å^3$, respectively. Data reduction and refinement formulae, anisotropic thermal parameters, and positional parameters of all atoms are available as supporting information.

(45) (a) SMART Area-Detector Software Package; Siemens Industrial Automation, Inc.: Madison, WI, 1993. (b) SAINT: SAX Area-Detector Integration Program; v. 4.024; Siemens Industrial Automation, Inc.: Madison, WI, 1995. (c) XPREP (v.5.03): Part of the SHELXTL Crystal-Structure Determination Package; Siemens Industrial Automation: Madison, WI, 1994. (d) TEXSAN: Crystal Structure Analysis Package; Molecular Structure Corporation, 1992. (e) Hai-Fu, F. SAPI91: Structure Analysis Programs with Intelligent Control; Rigaku Corp.: Tokyo, 1991. (f) Beurskens, P. T.; Admiraal, G.; Beurskens, G.; Bosman, W. P.; Garcia-Granda, S.; Gould, R. O.; Smits, J. M. M.; Smykalla, C. DIRDIF92: The DIRDIF Program System; Technical Report of the Crystallography Laboratory, University of Nijmegen, The Netherlands, 1992. (g) Creagh, D. C.; McAuley, W. J. *International Tables for Crystallography*; Kluwer Academic Publishers: Boston, 1992; Vol. C. (h) Ibers, J. A.; Hamilton, W. C. *Acta Crystallogr.* **1964**, *17*, 781.

Acknowledgment. The authors would like to thank Dr. Frederick J. Hollander, staff crystallographer at the CHEXRAY facility at the University of California, Berkeley, for performing the crystal structure determination of **1′** and for assisting with the other crystal structure determinations. The authors also thank Dr. Graham Ball for assistance with the ^{15}N-filtered ^1H spectra and the National Institutes of Health (Grant No. R37 GM25459) for financial support.

Note Added in Proof: While this work was in press, Boncella reported dimeric square-planar nickel amido dimers which react similarly with PMe_3 and have similar upfield NH resonances: VanderLande, D. D.; Abboud, K. A.; Boncella, J. M. *Inorg. Chem.* **1995**, *34*, 5319.

Supporting Information Available: Additional information on the collection, processing, and refinement of the X-ray crystal structures of *cis*-**1′**, *trans*-**3′**, and **4′**; anisotropic thermal parameters and positional parameters for all atoms in the X-ray crystal structures of *cis*-**1′**, *trans*-**3′**, and **4′**; and full tables of intramolecular distances and angles (13 pages). This material is contained in many libraries on microfiche, immediately follows this article in the microfilm version of the journal, can be ordered from the ACS, and can be downloaded from the Internet; see any current masthead page for ordering information and Internet access instructions.

JA952882L